Individualization of transcranial direct current stimulation based on individual motor function and anatomy in chronic stroke patients

Renée F. Dooren

TU Delft

Individualization of transcranial direct current stimulation based on individual motor function and anatomy in chronic stroke patients

By

Renée F. Dooren

in partial fulfilment of the requirements for the degree of

Master of Science
in Biomedical Engineering

at the Delft University of Technology,
to be defended publicly on Thursday August 26, 2021 at 10:00 AM.

Student number: 4221036

Thesis committee:		
	Dr. Ir. A. C. Schouten, supervisor	TU Delft
	Ir. J. van der Cruijsen, supervisor	Erasmus MC
	Prof. Dr. R. W. Selles, supervisor	Erasmus MC
	Dr. Ir. K. Batselier,	TU Delft

Preface

The work in front of you is the result of my thesis for an MSc title in Biomedical Engineering at the Delft University of Technology. This project was made possible by the rehabilitation department of the Erasmus MC and by the 4DEEG consortium; I would like to thank them for this opportunity. Secondly, I would like to thank Ruud Selles from the Erasmus MC and Alfred Schouten from the TU Delft for their supervision and suggestions on how to proceed with this project.
Although I wouldn't recommend anyone to graduate in a pandemic with a semi lockdown, I enjoyed working on this graduation project. The fact that I look back on it with pleasure is largely due to Joris van der Cruijsen and his great supervision. Joris, thank you for all the input you gave. Your ideas, feedback and encouraging words helped me to overcome the challenges faced during this project.

Furthermore, I would like to thank my parents for their unconditional support, my friends for the (sometimes a bit too much) fun distractions and comic relief, and of course Cees, just for being there for me.

Finally, I would like to share with you that I am proud of obtaining an engineering title exactly 70 years after my both grandfathers, Theo van der Pas and Jan Dooren, who obtained the same title in 1951 at the mechanical engineering faculty of the Technische Hogeschool Delft, the predecessor TU Delft.

Renée Dooren
Delft, August 2021

Abstract

Transcranial Direct Current Stimulation (tDCS) is an upcoming therapeutic tool to improve post-stroke upper extremity motor function by modulating cortical excitability. However, research shows mixed findings on tDCS in stroke patients. The functional and structural brain reorganization may explain the mixed findings: (i) The individual motor function, i.e. the target for tDCS, may be relocated to a non-affected brain region, and (ii) the structural characteristics, i.e. conductivity, of the lesion influences the current propagation in the brain.

This study evaluated the effect of individual optimized tDCS configurations for 21 chronic stroke patients and ten healthy controls using model simulations. We optimized tDCS configurations for two individual targets: (i) a functional target based on EEG during a functional hand task and (ii) an anatomical target based on MRI. The individual optimized configurations are compared with conventional configurations targeting the contralateral and ipsilateral primary motor cortex. The configurations are compared based on the normal component of the simulated electric field at both the functional and anatomical targets. Here we consider a negative field strength inhibitory, therefore undesirable.

The functional target was found ipsilateral in eight of the twenty-one stroke subjects, which indicates the relevance of individual functional targets. The conventional configurations simulated for all healthy subjects a positive field strength in the anatomical target. However, our simulations showed that conventional tDCS can result in negative stimulation for seven stroke subjects in the functional target and two stroke subjects in the anatomical target. The simulations may explain the lack of consistent therapeutic effects of conventional tDCS in stroke patients, and highlight the need for individualized tDCS configurations.

Contents

1. Introduction

A stroke is a cerebrovascular accident (CVA) in which brain cells die due to lack of blood flow (ischemic stroke) or due to bleeding (haemorrhagic stroke). It is the third most common cause of death, and the biggest cause of acquired motor impairment, worldwide (Gavaret et al., 2019). Motor impairment in stroke can be caused by injury to the motor cortex, premotor cortex, motor tracts, or associated pathways in the cerebrum or cerebellum(Langhorne et al., 2009). In the first months post-stroke, patients often recover 40 to 70% of their brain function(Siegel et al., 2018). This progress is caused by a brain-recovery mechanism: neuroplasticity. Neuroplasticity is a lifelong ongoing process with the ability to change and adapt the brain as a result of experiences or brain injuries. These adaptations can be, e.g. the strengthening or weakening of synapses over time or the relocation of a certain brain function to a non-affected brain area. However, despite the neuroplasticity, the complete motor recovery rate in stroke patients is poor. In research is stated that in six months after stroke, seven out of eight patients do not achieve complete motor recovery(Lefebvre & Liew, 2017). To improve this recovery rate, there is a need for new and improved therapeutic tools.

Transcranial Direct Current Stimulation (tDCS), a form of non-invasive brain stimulation (NIBS), has therapeutic potential for psychiatric conditions and brain injuries. TDCS can modulate cortical excitability, which results in neuroplastic changes (neuroplasticity) (Laakso et al., 2019; Rozisky et al., 2016). TDCS can stimulate or inhibit targeted brain regions to modulate its neural plasticity by applying a weak (0.5-2 mA) direct current through electrodes on the scalp(Lefebvre & Liew, 2017). The higher the electric field strength a targeted brain region is exposed to, the more likely the brain region's cortical excitability is modulated(Antonenko et al., 2019; Caulfield et al., 2020; Datta et al., 2012). Therefore, to stimulate motor recovery with tDCS, it is important to precisely target the brain area with a sufficiently high electric field strength. The electric field strength in the targeted brain area after tDCS depends on (i) the tDCS configuration, i.e., the position, size, amount, current intensity and locations of the electrodes, and (ii) the structural characteristics of the subject's head, such as the different tissues' conductivities, volumes and locations.

As a neurorehabilitation tool, tDCS seems a viable technique due to the limited side effects and the safety aspects (characteristic of non-invasive brain stimulation techniques). Another important benefit of tDCS is its availability, relative affordability, and the technique is simple in application. These benefits are a reason for the increased research on the effects of tDCS. However, research shows mixed findings on the effect of tDCS on motor rehabilitation in stroke patients(Laakso et al., 2019; Lefebvre & Liew, 2017; Vliet et al., 2017). Various clinical studies implemented tDCS to modulate motor excitability in stroke patients, wherein some studies demonstrate that 50% or more of the stroke patients fail to show response to the tDCS.

Some of the mixed findings reported in clinical tDCS studies on improving motor function in stroke patients may be explained by the variability in stroke lesions (Lefebvre & Liew, 2017). Structural reorganization caused by the lesion properties such as volume, location and conductivity varies between individuals and influences how current passes through the brain (Minjoli et al., 2017). The tDCS aims to stimulate a brain target to modulate the cortical excitability, but the target is not always reached optimally due to the structural reorganization. Furthermore, individual motor function, dependent on stroke severity and consequent recovery, is another source of variability in chronic stroke patients: functional reorganization may occur, i.e. individual motor function may be relocated to a non-affected brain region(Nitsche et al., 2015; Rich & Gillick, 2019). Ignoring the functional and structural reorganizations when designing tDCS configurations (electrode locations and applied currents) to enhance motor recovery in chronic stroke patients may lead to suboptimal stimulation, i.e., current not maximally reaching the targeted brain regions. It is currently unknown to what extent individualization based on structural and functional variability is required for optimal stimulation.

This study aims to determine if individual optimized tDCS configurations show higher and more consistent electric field strengths in the targeted brain area after simulation of tDCS, compared to conventional configurations. We do this by comparing the simulated electric field strength in a functional and an anatomical targeted brain region after stimulation with conventional and individual optimized tDCS configurations. Both the conventional and individual optimized configurations consist of two electrodes. In this study, the tDCS is simulated in individual MRI based head models,

with the structural characteristics of the lesion considered. The individual optimized configurations are optimized for maximal stimulation at two different targets. (i) A functional target based on EEG during a functional hand task and (ii) an anatomical target, i.e. the location of the motor hand knob based on MRI. In the individual optimized configuration for the anatomical target, the structural reorganization is taken into account. For the functional target, both the structural and functional reorganizations are considered. Furthermore, an analysis is done with individual optimized tDCS configurations of 2, 4, 6 and 8 electrodes: new techniques with smaller electrodes allow applying tDCS with multiple electrodes (Dmochowski et al., 2011), which could be beneficial in individualization.

In the methods section (Section 2), a summary of the relevant methods of the used input is described. The methods section also includes the methods applied in this study, e.g. for determining the anatomical tDCS targets and the use of SimNIBS for the optimization to the functional and anatomical tDCS target and the simulation of conventional tDCS configurations. The third chapter is concerned with the results, followed by the discussion and limitations in chapter four. The last chapter presents the conclusion of this thesis.

2. Methods

This study is partly based on data gathered prior to this study. The MRIs and EEG data of twenty-one stroke patients and ten healthy subjects were collected in a study from the 4D-EEG consortium(Vlaar et al., 2017). The subject-specific head models and the functional tDCS targets based on EEG source localization were also given beforehand. Figure 1 shows a flowchart with the different steps and processes relevant to this study. The figure also indicates what steps are completed prior to this study.

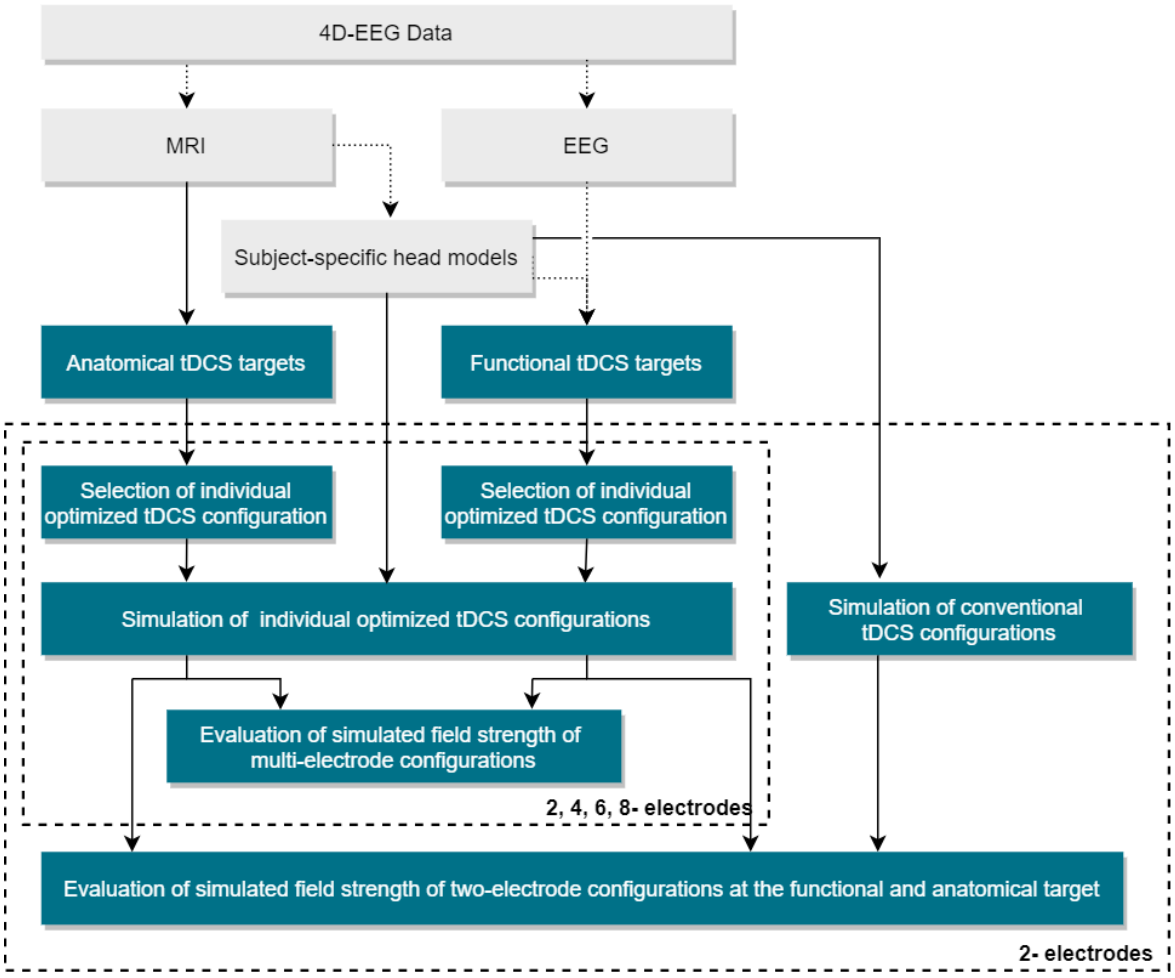

Figure 1. Flowchart of process steps of this thesis. The light grey blocks are steps taken on beforehand of this study and used as input. The blue blocks are the process steps of this study. Individual optimized configurations are selected, simulated and evaluated for configurations with 2, 4, 6 and 8 electrodes. The evaluation and comparison of the individual optimized and conventional configurations are only done for the 2-electrode configurations. The number of electrodes in the evaluations are indicated by the frames with dashed lines.

2.1. Data collection

A full description of the participants and the experimental design for collecting EEG and MRI was described in the study of Vlaar et al., 2017. Prior to this study, the EEG data were preprocessed. Subject-specific head models were built (section 2.2.1), and individual functional tDCS targets were determined with EEG source localization (section 2.2.2.1). Here, we summarise the methods of the prior work relevant to the current study. Furthermore, the methods of work done in this study are described.

2.1.1. Participants

We included data from twenty-one chronic hemiparetic stroke subjects at 47 ± 35 (mean ± standard deviation) months after stroke, aged 48 to 77 years (Table 1). As a control group, we included ten age-matched healthy subjects (average age: 51 to 75 years). The data were previously collected as part of the 4D EEG study (Vlaar et al., 2017) and was approved by the Medical Ethics Reviewing Committee of the VU Medical Centre, Amsterdam.

2.1.2. Robotic manipulator

A robotic wrist joint manipulator continuously perturbed the impaired wrist of the hemiparetic stroke patients and the dominant right hand of the healthy controls during a passive and active task. During the tasks, EEG was recorded as described in 2.1.3. These data were used for EEG source localization to define a functional tDCS target, see 2.2.2.1. In the the passive task, participants were instructed to ignore the applied disturbances and relax their wrist while holding the handle of the robotic manipulator. The applied disturbances elicit sustained oscillatory responses in the EEG, also known as steady-state responses. During the active task, the robotic manipulator exerted the same continuous perturbations, but subjects had to maintain a wrist flexion torque of 20% of the maximum voluntary contraction (MVC). The MVC was determined per subject for the perturbed arm, while the participants were verbally encouraged to perform wrist flexion with maximal effort.

Table 1. *Patients characteristics*

ID	Age (years)	Sex	Affected hand side	Time post-stroke (months)	FMA	EmNSA					
						LT	P	PP	D	PR	Total
1	64	M	L	82	13	8	8	8	8	8	40
2	62	M	R	49	39	8	8	8	8	8	40
3	77	M	L	7	62	6	8	8	6	6	34
4	66	F	R	212	9	2	3	4	-	0	9
5	76	F	L	35	63	8	8	8	5	8	37
6	54	M	L	21	8	0	2	3		4	9
7	67	M	R	26	54	8	8	8	7	8	39
8	55	M	L	75	58	8	8	8	8	8	40
9	59	M	L	70	9	6	8	8	4	8	34
10	68	F	R	67	66	8	8	8	8	8	40
11	49	F	L	40	59	8	8	8	8	8	40
12	57	M	L	9	66	8	8	8	8	8	40
13	48	M	L	80	10	5	8	8	4	8	33
14	65	M	L	22	64	8	8	8	4	8	36
15	50	F	R	52	59	7	8	8	4	8	35
16	50	M	R	33	48	8	8	8	8	8	40
17	56	M	L	8	56	8	8	8	6	8	38
18	48	M	R	88	66	8	8	8	8	8	40
19	61	F	R	10	60	8	8	8	7	8	39
20	72	M	L	15	26	3	7	4		6	20
21	68	M	L	142	20	3	3	5		4	15

Note. Sex (F: female, M: male); Affected hand side (L: left, R: right); FMA: Fugl-Meyer Assessment; EmNSA: Erasmus MC Modifications to the Nottingham Sensory Assessment; LT: light touch; P: pressure; PP: pinprick; D: discrimination; PR: proprioception.

Due to the limitations of the robotic manipulator, the maximum torque level for the active task was set to 4 Nm. Three healthy subjects had a 20% MVC higher than 4 Nm.

Participants always performed the passive task before the active task. If a participant was not capable of voluntary wrist flexion, the active task was not performed. Participants performed 20 trials of 12.5 seconds for each task. The perturbance signal had a periodicity of 1.25 seconds, such that a single trial consisted of 10 repetitions of the same perturbation.

2.1.3. EEG

EEG was recorded during the passive and active task with 62 Ag/AgCl electrodes (TMSi, the Netherlands) arranged according to the international 10/10 system (R Oostenveld & Praamstra, 2001) using a biosignal amplifier (Refa128, TMSi). All data were recorded at 2048 Hz, with only an anti-aliasing filter. A snap-on electrode at the left mastoid served as the ground electrode. The impedance of all EEG electrodes was ensured to be below 20 kOhm before the experiment started. In addition, the position of all electrodes, the nasion and the left and right ear were digitized for co-registration with the MRI (see next section).

2.1.4. MRI

Structural T1w MRIs of each participant were acquired at the VU Medical Center, Amsterdam, using a Discovery MR750 3 T scanner (GE, Waukesha, WI, USA) with a 3D fast spoiled gradient-recalled-echo sequence, consisting of 172 sagittal slices (256 x 256), using the following acquisition parameters: TR = 8.208 ms, TE = 3.22 ms, inversion time = 450 ms, flip angle = 12°, voxel size 1 x 0.94 x 0.94 mm (Vlaar et al., 2017). Locations of the nasion and the left and right ear were manually identified on the MRI image to allow alignment of the EEG cap.

2.2. Data processing

2.2.1. Subject-specific head models

Individual finite element volume conductor models of stroke subjects were created as described by (Piastra et al., 2021) to both perform EEG source localization and tDCS optimization and simulation. The T1-weighted MRI recording was first segmented using SimNIBS 3.2 (Simulation of Non-Invasive Brain Stimulation), (Saturnino et al., 2018; Thielscher et al., 2015) into a 6-tissue finite element head model consisting of scalp, eyes, skull, cerebrospinal fluid (CSF), grey matter (GM) and white matter (WM). We used the standard conductivity values of SimNIBS: 0.465 S/m for the scalp, 0.5 S/m for eyes, 0.01 S/m for the skull, 1.654 S/m for CSF, 0.275 S/m for grey matter and 0.126 S/m for white matter.

We want to optimize individual tDCS configurations on head models in stroke patients; therefore, the inclusion of lesion tissue in the head model is necessary. Since SimNIBS only identifies healthy tissue, the LINDA algorithm (Pustina et al., 2016) was used to segment the lesion for each patient. Both segmentations were combined into a single, 7-tissue model, in which the lesion voxels from LINDA are replacing the overlapping white matter/grey matter/CSF elements generated by SimNIBS. The conductivity of the lesion tissue in SimNIBS was set to 1.654 S/m, the same as CSF.

2.2.2. Stimulation targets

The target brain area for tDCS was the brain area that we aimed to excite, to stimulate recovery. We have determined individual targets on which we optimized the individual tDCS configurations. Furthermore, we used the targets to evaluate the simulations of the individual optimized configurations and the conventional configurations by comparing the electric field strength at the target.

We have used two different targets: a functional target and an anatomical target. We made for each participant for both targets optimized tDCS configurations. The functional target is defined using EEG and may be located outside the motor cortex or ipsilateral due to the functional reorganization. The conventional configuration is designed to stimulate the motor cortex. If the functional target is outside the motor cortex, then the conventional configuration is expected to be less effective in reaching the target, i.e., a lower field strength. If we compare the field strengths in the functional target after simulation of the individual optimized configuration for the functional target and the contralateral conventional configuration, we study the influence of structural and functional

reorganization on the intensity of the field strength generated by conventional and individual optimized tDCS. We are also interested in the effect of only structural reorganization on tDCS, i.e. the effect of the lesion on the brain conductivity and current propagation. If we compare the field strength in the anatomical target after stimulation with the individual optimized configuration for the anatomical target and the contralateral conventional configuration, we study the influence of the structural reorganization while neglecting the functional reorganization. The functional tDCS target, described in section 2.2.2.1, was determined prior to this study. The anatomical tDCS target is determined in this study, and the methods are described in 2.2.2.2.

2.2.2.1. Functional tDCS targets.

The individual motor functional tDCS targets were defined using the EEG recorded during the robotic wrist manipulator task (see 2.2.1 and 2.2.2). All EEG data were preprocessed offline using Matlab (The Mathworks, Inc., USA), EEGLAB v14 toolbox (Delorme & Makeig, 2004) and Fieldtrip (Robert Oostenveld et al., 2011). First, the data were zero-phase bandpass filtered (0.5 to 40 Hz, FIR filter, order: 1691 and 87, respectively). The data were visually inspected to identify and remove noisy channels from the data, and then the data was re-referenced back to the common average. On average, 3.1 channels were removed from the data. Next, the passive and active trials were divided into 1.25-second epochs according to the perturbation signal periodicity. Noisy epochs were visually identified and discarded from the data. Not all stroke subjects were able to complete all trials of the active task. On average, 136 (range: 84 to 184) and 124 (range: 0 to 206) trials remained for the passive and active task for the stroke patients, respectively. For the healthy subjects, 133 (range: 99 to 182) and 144 (range: 96 to 177) of the passive and active task were included for the subsequent processing steps, respectively.

In the next step, extended infomax independent component analysis (ICA, (Bell & Sejnowski, 1995; Makeig et al., 1996)) was applied to the combined passive and active EEG data. Components corresponding to eye blink or muscle artefacts were visually identified based on their power spectra and topographic activation and consequently discarded from the analysis.

Source localization was performed on the remaining independent components to determine the brain region responsible for generating the recorded scalp activity. The individualized finite element head model (see 2.2.1) was used to fit equivalent dipoles to the independent components. A single dipole location engaged in motor control as a functional tDCS target was identified based on two criteria. First, the residual variance of the dipole had to be below 10% (Delorme et al., 2012). Second, compared to the power spectrum of passive trials, active trials should show a reduction in alpha (8 to 12 Hz) and beta (14 to 30 Hz) power, reflecting active motor control (Pfurtscheller et al., 1996). If multiple dipoles fulfilled these criteria, the dipole closest to the ipsilesional motor cortex was selected as a functional tDCS target.

2.2.2.2. Anatomical tDCS targets.

This anatomical tDCS target is based on the location of the hand knob in the motor cortex, determined on individual anatomy in the MRI. We identified the contralateral hand knob following (Huber, 2018): the motor cortex has an inter-subject consistent folding pattern, with a small variety of typical hand-knob structures. By manually and visually inspecting the MRIs of all subjects, the hand-knob locations' coordinates on the motor cortex were determined. The anterior side of the hand knob was used as an anatomical tDCS target location (Jaillard et al., 2005). The hand knob could not be found in two stroke subjects due to the lesion; those subjects were not included in this analysis.

2.2.3. Selection and simulation of tDCS configurations

SimNIBS 3.2 (Saturnino et al., 2018; Thielscher et al., 2015) was used to optimize individualized tDCS configurations for maximal field strength in the E normal component at the individual functional and anatomical targets for all subjects. Furthermore, we used SimNIBS to simulate the conventional configurations. All optimizations and simulations were applied on the subject-specific head model (section 2.2.1). For all simulations and optimizations, the standard conductivity values of SimNIBS were used; 0.126 S/m for white matter, 0.275 S/m for grey matter, 1.654 S/m for CSF, 0.01 S/m for the skull and 0.465 S/m for the scalp (Thielscher et al., 2015). We

used 1.654 S/m as conductivity for lesion tissue, the same as CSF. We defined the electrodes as 5mm radius circular shape and 3mm thickness (Saturnino et al., 2019) and used the subset of 80 electrode positions of the EEG10/10 system.

2.2.3.1. Simulation for conventional tDCS configurations

We used SimNIBS to simulate the conventional configuration targeting the motor cortex, i.e. an anode on the contralateral M1 (C3 or C4, (Nitsche & Paulus, 2000; Rich & Gillick, 2019)) and a cathode on the ipsilateral supraorbita (Fp2 or Fp1, (Fischer et al., 2017)). We set the applied current on the anode at 2mA(Lefebvre & Liew, 2017; Saturnino et al., 2019).

The contralateral conventional configuration would be applied on stroke subjects when no functional or structural reorganization is considered. We do consider these reorganizations, which results in ipsilateral functional targets for some subjects. Therefore, we simulate both contralateral and ipsilateral conventional configurations. This way, we can analyze if the ipsilateral conventional configuration performs better in ipsilateral functional targets than the contralateral conventional configurations.

2.2.3.2. Optimization of individual tDCS configurations for all targets

The individual optimized configurations are optimized for maximal field strength in the E normal component at the individual functional and anatomical targets. The E normal component is defined orthogonally to the middle later of the grey matter (Antonenko et al., 2019). Instead of the norm, the normal component of the electric field was used because transcranial current stimulation is believed to work through stimulation of the pyramidal neurons, which are oriented normal to the cortical surface(Das et al., 2016). SimNIBS uses a surface mesh of the middle layer of the grey matter for these E normal computations. However, SimNIBS created this mesh without considering the lesion. We have included the segmentation of the lesion tissue in this middle layer grey matter mesh in the same way as in section 2.2.1 (Piastra et al., 2021). The MATLAB code is included in appendix V. SimNIBS could not directly use this modified mesh. Therefore we have altered a part of the source code of SimNIBS, see appendix III.

The first step of the tDCS optimization was the calculation of the lead field. The lead field was calculated by placing all the electrodes on the head model and then calculating the electric field in the brain caused by each electrode.

With the calculated lead fields, tDCS configurations can be optimized to maximally stimulate a 2 mm radius sphere centred around the functional or anatomical target. SimNIBS always optimizes towards a node in the mesh of the head model. Therefore, the node in the model closest to the functional or anatomical target coordinates is used to optimize stimulation intensity.

Optimization was performed for maximally 2, 4, 6 and 8 electrodes of the standardized 10/10 system with a maximum current per individual electrode set to 2 mA (Lefebvre & Liew, 2017; Saturnino et al., 2019), which gives the maximum total current as 2, 4, 6 and 8 mA. The 2-electrode individual optimized configurations were used to compare the conventional configurations, which also consists of 2 electrodes. The individual optimized configurations for multiple electrode pairs were used to indicate the future potential of individualized tDCS. New techniques with smaller electrodes allow applying tDCS with multiple electrode pairs (Dmochowski et al., 2011), which could be beneficial in individual optimized tDCS configurations: optimized multi-electrode stimulation can increase the focality and intensity at the target.

2.3. Analysis

2.3.1. Identified targets

We compared the functional and anatomical target locations for the subjects for whom we defined a contralateral functional target and an anatomical target. We compared the minimum, maximum and median of the total distance in mm ($\sqrt{x^2 + y^2 + z^2}$) and the distances in the x-, y- and z-direction between the functional and anatomical target. We did this separately for the stroke subjects and healthy subjects.

2.3.2. Electric field strength

2.3.2.1. Individual optimized tDCS configurations vs conventional

We compared the simulations of the conventional configurations with the individual optimized configurations, one for each target, by the simulated electric field strength at the functional or anatomical target. The conventional configuration would be applied to stroke patients when no structural or functional reorganization is considered. In selecting the individual optimized configuration for the anatomical target, the structural reorganization is considered, by means of the subject-specific volume conductor model where the lesion tissue is taken into account. The individual optimized configuration for the functional target is selected considering both structural and functional reorganization, since the target is determined based on EEG. By comparing the field strengths of the conventional and individual optimized configurations, we can evaluate the effects of the structural and functional reorganization on the electric field in stroke patients on tDCS.

We used the E normal component of the field strengths for the comparison. We extract the average normal E electric field in a 2mm sphere centred around the grey matter node closest to the functional or anatomical target coordinate. This field strength is used to evaluate and compare the configurations.

We assumed a high and positive E normal field strength to have the desired tDCS effect. A positive E normal field strength is directed inwards to the cortex and is considered stimulating. A negative E normal field strength is directed outwards of the cortex and is considered an inhibiting effect. Therefore, we are interested in configurations with a positive E normal field strength at the functional and anatomical target. Furthermore, previous research showed a positive link between simulated field strength and empirically assessed brain stimulation effects: the higher the field strength, the more likely the brain's cortical excitability is modulated(Antonenko et al., 2019; Datta et al., 2012). However, there is no known threshold for a stimulation dosage that is sufficient to induce physiological effects(Caulfield et al., 2020). In our analysis we note when a simulated field strength is very low, expecting that this field strength may induce no physical effect. However, since there is no known threshold, we do not quantify this.

We compare the field strength in the functional and anatomical targets separately. The stroke subjects and healthy subjects are also evaluated separately. Furthermore, we evaluate the absolute difference and the relative difference between the contralateral conventional and individual optimized configurations. The relative difference is a unitless value, calculated per subject and target by subtracting the field strength at the target of the contralateral conventional configuration from the field strength of the individual optimized configuration, divided by the absolute field strength of the contralateral conventional configuration. With this, we evaluate the difference in effectiveness on field strength between the conventional and individual optimized configurations.

2.3.2.2. Functional vs anatomical tDCS targets

2.3.2.2.1. Comparison of field strengths in functional and anatomical targets

We are interested in the difference in electric field strength between the individualized configurations optimized to a functional or an anatomical target. To do so, we compared the relative difference in the functional and the anatomical target between the contralateral conventional configuration and the individual optimized configurations. With this comparison, we study the difference in influence of considering only the structural characteristics, or both the structural and functional reorganization.

Furthermore, we provide an overview of the number of subjects, per subject group and type of target, that are stimulated with the contralateral conventional configuration and who of them are stimulated (positive field strength), inhibited(negative field strength) or have a negligible field strength (low field strength). We do this to study whether stroke subjects or healthy subjects in the functional or anatomical target are suitable for implementing the conventional tDCS configuration. We are interested in the number of cases for whom this applies or who would benefit from an individual optimized configuration.

2.3.2.2.2. Comparison of electrode configurations

We compare the locations of the anodes in the 2-electrode optimized configurations of the anatomical and individual target. We mirror all individual configurations for the subjects with a functional or anatomical target from the right to the left hemisphere. This way, we can compare the configurations of all the subjects. We do this separately for the stroke and healthy subjects and separately for the anatomical and functional targets. For the individual optimized configurations for the anatomical target, we expect to see anode locations similar to the conventional configuration for both stroke subjects and healthy subjects. We expect to see more variance in electrodes used in anodes for the functional target since there is more variance in the target location.

2.3.2.3. The effect of an increased number of electrode pairs.

We did an additional analysis to show the added value of multi-electrode tDCS configurations, compared to a two-electrode tDCS configuration. Previous research is often done with large electrodes to apply tDCS. More recent studies included tDCS applied via smaller electrodes. These smaller electrodes allow for the use of multiple electrode pairs in tDCS, which may lead to an increase in focality and intensity of the electric field strength at the target(Dmochowski et al., 2011, 2013). We analyzed the increase in field strength, with an increase of electrode pairs: 2, 4, 6 and 8 electrodes.

3. Results

3.1. Identified tDCS targets

3.1.1. Functional tDCS targets

The identified functional tDCS targets (described in section 2.2.2.1) for the twenty-one stroke subjects were twelve times located in the contralateral hemisphere, eight times in the ipsilateral hemisphere. For one subject, we could not identify a functional target based on the EEG. As an example, the functional targets found by equivalent dipole fitting for two stroke subjects are shown in Figure 2.

For the healthy subjects, no functional target was found for two subjects, and the functional targets found for the other subjects were located in the contralateral hemisphere. An overview of all the subjects' targets can be found in Appendix A.

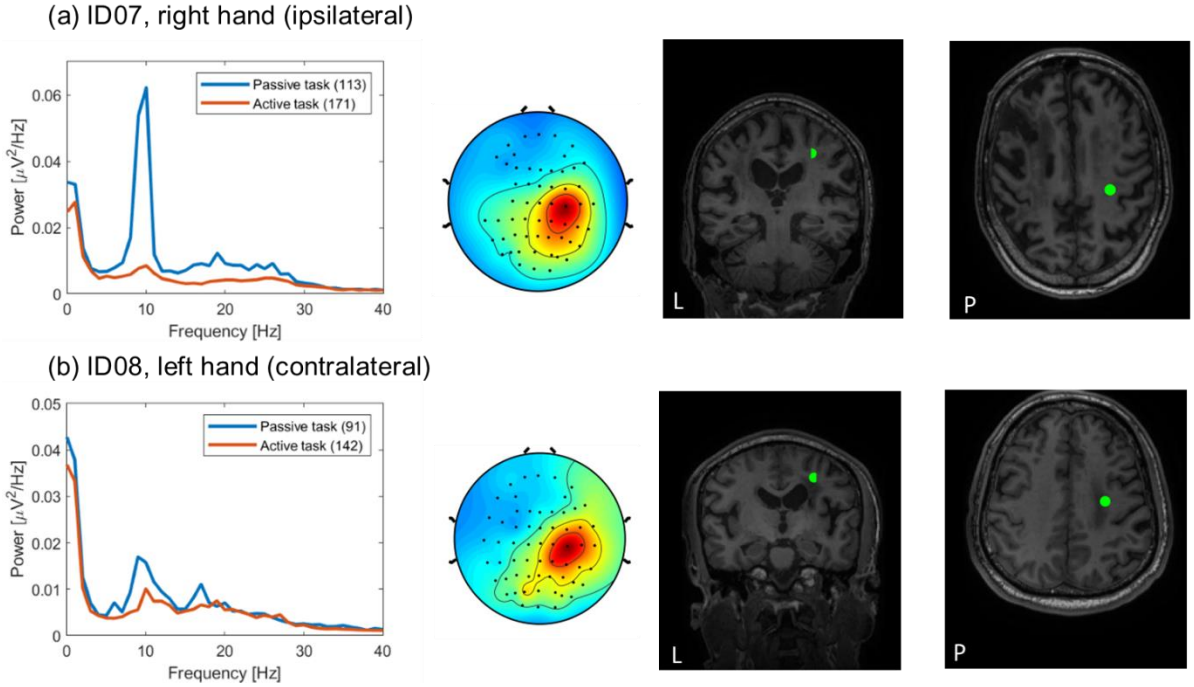

Figure 2. The functional tDCS target is based on equivalent dipole fitting on EEG for two stroke subjects. (ID07, ID08) Left: the power spectrum of the equivalent dipole used as functional target (left). The blue line represents the power spectrum of the trials of the passive tasks; the orange line represents the trials of the active task. Middle: the scalp map of the equivalent dipole. Right: the equivalent dipole location is shown with a green marker in individual MRI. 'L' indicates left, 'P' indicates posterior. ID07's right hand is impaired, the functional target is found ipsilateral. ID08's left hand is impaired, the functional target is found contralateral.

3.1.2. Anatomical tDCS targets

The anatomical tDCS target was not found for two stroke subjects (ID04, ID13) due to a lesion at that location. Nevertheless, we can mention something about the subjects with no anatomical target: those two stroke subjects have an ipsilateral functional target. For all other participants, the anatomical tDCS target was found. All subjects' coordinates for both targets and whether they are contra- or ipsilateral can be found in Appendix A.

3.1.3. Comparison of locations of the functional and anatomical tDCS targets

The locations of the functional and anatomical targets are, per subject, in all cases different. To compare the different locations per subject, we only consider subjects for whom a contralateral functional target and an anatomical target are found. That is the case for twelve stroke subjects and eight healthy subjects. The median distances between both targets are similar in stroke subjects (median: 19.88 mm, range: 6.49-36.87 mm) and healthy subjects (median: 20.94 mm, range: 11.73 –

41.21 mm). All distances per direction (x,y,z) and total distances can be found in Appendix B. This appendix also presents the min, max and median (absolute) distances.

3.2. Electric field strength

In sections 3.2.1. to 3.2.3.2. the results of the simulations of the 2-electrode individual optimized tDCS configurations are presented. The field strengths of the individual optimized and conventional configurations in the functional and anatomical target can be found in Appendix A. The multi-pair individual optimized configurations simulations are presented in the last section of this chapter (3.2.4.)

3.2.1. Functional tDCS targets

The contralateral conventional configuration simulates a negative E normal electric field strength in the functional tDCS target of seven of the twenty stroke subjects with a functional target (median: 0.02 V/m, range: -0.32 – 0.32 V/m) and one of the eight healthy subjects (median: 0.18 V/m, range: -0.12 – 0.40 V/m), see the top panel in Figure 3. Three of these stroke subjects with a negative field strength have an ipsilateral functional target (IDs: 04, 13, 14) and four a contralateral functional target (IDs: 09, 10, 17, 18). Furthermore, the other five stroke subject with an ipsilateral functional tDCS target have a positive electric field strength after simulation of the contralateral conventional configuration(IDs: 05, 07, 15, 19, 20). These positive and negative field strengths imply that the direction of the field is unpredictable when applying contralateral conventional tDCS while the functional target is ipsilateral.

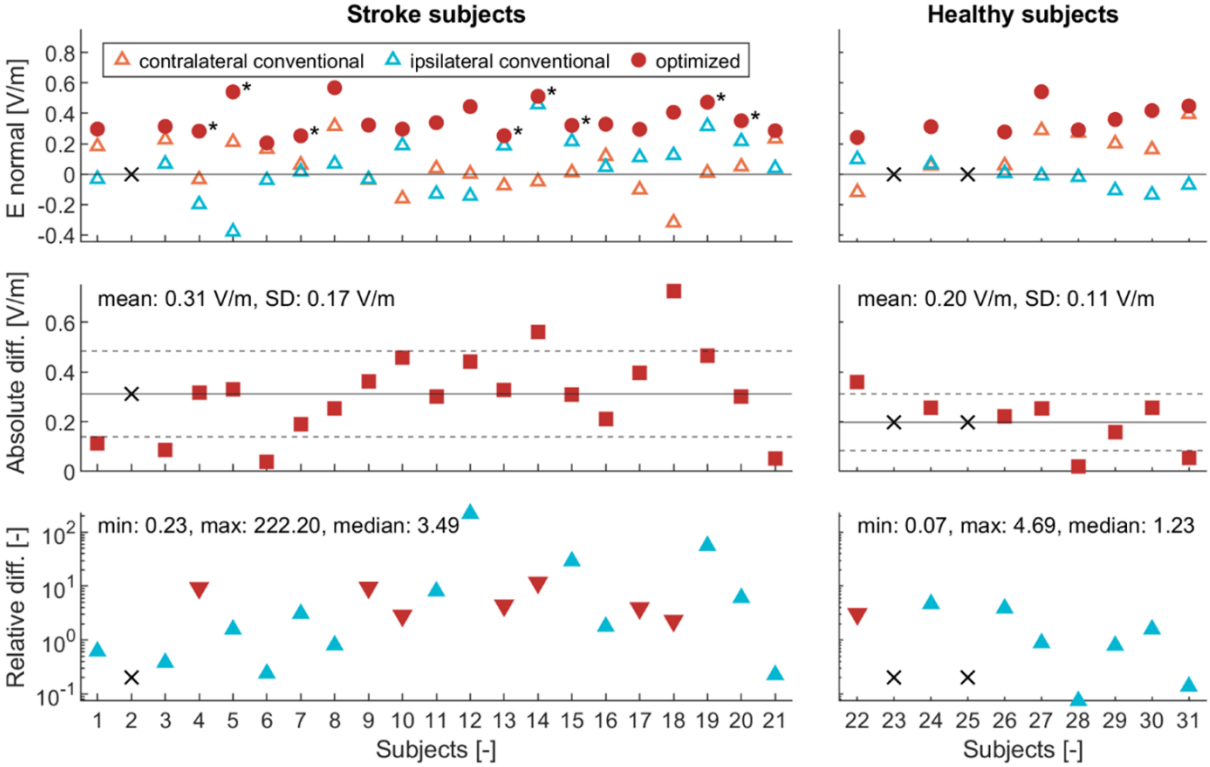

Figure 3. The field strength at the functional tDCS target. Top panel; electric field strength of E normal component at a 2mm radius sphere around functional target per subject in different configurations; the red circle is the marker for the individual optimized 2-electrode configuration; the orange triangle represents the contralateral (ipsilesional in stroke patients) conventional configuration, and the blue triangle the ipsilateral conventional configuration. The individual optimized 2-electrode configuration can be contra- or ipsilateral: subjects with an induvial optimized configuration targeting ipsilateral are marked with an asterisk. Central panel; the absolute difference between the individual optimized 2-electrode configuration and the contralateral conventional configuration. Bottom panel: the relative difference between individual optimized 2-electrode configuration and contralateral conventional configuration. (optimal – contra.)/abs(contra.) The red ▼ marker indicates a negative field strength for the contralateral conventional configurations, thus inhibiting tDCS. The X-markers represent the subjects whose functional tDCS target is not found (ID02, ID23, ID25).

If we look at ID05, this subject's functional target is ipsilateral. However, the ipsilateral conventional configuration produces a negative electric field strength, while the contralateral configuration results in a positive electric field strength. ID04 and ID09 have a negative field strength for both conventional configurations and have respectively an ipsilateral and contralateral functional tDCS target.

The individual optimized 2-electrode configuration results in the functional target in positive and higher field strength for all stroke subjects (median: 0.32 V/m, range: 0.21 – 0.57 V/m) and healthy subjects (median: 0.34 V/m, 0.24 – 0.54 V/m) than the conventional configuration. The simulated field strengths for the individual optimized configurations indicate that all stroke subjects are stimulable with tDCS for the functional target, despite the low field strength for some subjects in the conventional configurations.

The middle panel of Figure 3 shows the absolute difference between the individual optimized 2-electrode configuration and the contralateral conventional configuration. The mean absolute difference and the standard deviation in stroke subjects (0.31±0.17 V/m) are higher than in healthy subjects (0.20±0.11 V/m). The functional and structural reorganization may explain this higher mean absolute difference in stroke patients: the median field strength simulated with the contralateral conventional configuration is lower in stroke subjects (0.02 V/m) compared to healthy subjects (0.18 V/m), while the median field strength simulated with the individual optimized configurations are more similar (respectively 0.32 V/m and 0.34 V/m).

The relative difference (see bottom panel of Figure 3) for ID12 and ID19 is large due to the small electric field strength of the contralateral configurations of both subjects (respectively 0.002 and 0.008 V/m). The median relative difference in higher in stroke subjects (median: 3.49, range: 0.23 – 222.20) compared to healthy subjects (median: 1.23, range: 0.07 – 4.69)

Two stroke subjects as an example to visualize and compare the effect of conventional and individual optimized tDCS configurations can be seen in Appendix F. The field strengths of the E normal component are visualized. The optimized configurations show a higher and better-targeted field strength at the functional tDCS target than conventional configurations. In ID07, the individual configuration consists of two electrodes on one hemisphere, which results in less electric activity in the not-targeted brain.

3.2.2. Anatomical tDCS targets

The anatomical tDCS targets for the contralateral conventional configurations have a negative (inhibiting) E normal electric field strength in two stroke subjects (ID10, ID12); all the other stroke subjects for whom an anatomical target was found have a positive field strength for the contralateral conventional configuration (median: 0.10 V/m, range: -0.04 – 0.25 V/m), see top panel of Figure 4. All healthy subjects are stimulated with a positive field strength in the anatomical target in the simulation of the contralateral conventional configuration (median: 0.18 V/m, range: 0.06 – 0.40 V/m).

The individual optimized 2-electrode configuration results in the anatomical target in a positive and higher field strength than the conventional configuration for all stroke subjects (median: 0.29 V/m, range: 0.13 – 0.40 V/m) and healthy subjects (median: 0.36 V/m, 0.20 – 0.54 V/m).

The ipsilateral conventional configuration simulates a negative field strength in all stroke subjects, except for IDs 16, 20 and 21 (median: -0.06 V/m, -0.17 – 0.08 V/m). The ipsilateral conventional configuration in healthy subjects only simulates negative field strengths (median: -0.08 V/m, range: -0.13 – -0.05 V/m).

The mean of the absolute difference is higher in stroke subjects (0.18±0.10 V/m) than in the healthy subjects (0.15±0.10 V/m); see middle panel Figure 4. The median of the field strength of the contralateral conventional and individual optimized configurations are higher in healthy subjects (0.18 and 0.36 V/m) than in stroke subjects (0.10 and 0.29 V/m). However, the difference between these contralateral conventional and individual optimized configurations medians is similar, explaining the similar mean absolute difference between healthy and stroke subjects. These results may imply that stroke subjects due to the structural reorganization are less stimulable at the anatomical target than healthy subjects. However, the relative difference (see bottom panel Figure 4) shows that it is more

beneficial to apply individual optimized configurations for stroke subjects (median: 1.98, range: 0.20 – 114.67) than healthy subjects (median: 0.62, range: 0.13 – 5.52).

The negative electric field strength of the contralateral conventional configuration is also visualized in the relative difference plot (bottom of Figure 4), indicated by the red downwards pointing triangles. The relative difference for ID09 is large due to the small electric field strength of the contralateral conventional configuration of this subject (0.00 V/m), which is expected to have a negligible stimulating effect. The other subjects with a low (<0.02 V/m) absolute field strength for the contralateral conventional configuration are subjects ID03, ID06 and ID16.

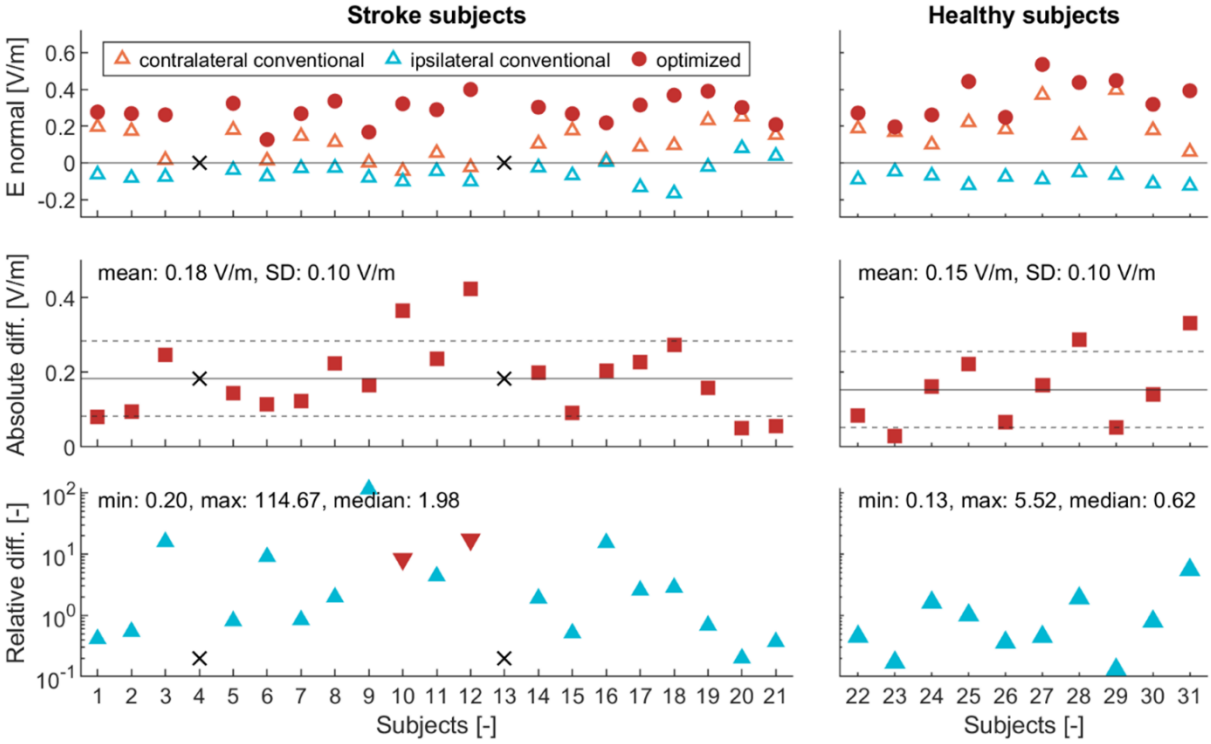

Figure 4. The field strength at the anatomical tDCS target. Top panel; electric field strength of E normal component at a 2mm radius sphere around anatomical target per subject in different configurations; the red circle is the marker for the individual optimized 2-electrode configuration; the orange triangle represents the contralateral conventional configuration, and the blue triangle the ipsilateral conventional configuration. Central panel; the absolute difference between the individual optimized 2-electrode configuration and the contralateral conventional configuration. Bottom panel: the relative difference between individual optimized 2-electrode configuration and contralateral conventional configuration. The red ▼ marker indicates a negative field strength for the contralateral conventional configurations, thus inhibiting tDCS. The X-markers represent the subjects whose functional tDCS target is not found (ID04, ID13).

Two stroke subjects as an example to visualize and compare the effect of the conventional and individual optimized tDCS configurations in the anatomical target are shown in Appendix G. The field strengths of the E normal component are visualized. The optimized configurations show a higher and better-targeted field strength at the functional tDCS target than conventional configurations. In ID07, the individual configuration consists of two electrodes on one hemisphere, which results in less electric activity in the not-targeted brain.

3.2.3. Functional vs Anatomical tDCS targets

3.2.3.1. Comparison of field strengths of functional and anatomical targets

Stimulating with individual optimized tDCS configurations results in a larger increase in field strength between the conventional and individual optimized configurations in the functional target than the anatomical target. This increase is, on average, also larger in stroke subjects than healthy subjects. We can compare this with the median relative differences, as presented in 3.2.1 and 3.2.2. The median relative difference for the healthy subjects is 0.62 for the anatomical target and 1.23 for

the functional target: the median relative difference is doubled for the functional target, compared to the anatomical target. For stroke subjects, the median relative difference for the anatomical target is 1.98, and for the functional target 3.49, more than a factor 1.75 higher. The contralateral conventional field strengths mainly cause this increase in median relative difference between the two types of targets. These field strengths greatly influence the relative difference since the relative difference results from the division by this field strength.

The contralateral conventional configuration often results in a negative field strength for stroke subjects' functional and anatomical targets. Appendix A presents all the field strengths per target and per configuration. These field strengths are also summarized in Figure 5. Negative field strengths are found after stimulation of the contralateral conventional configuration in the anatomical target of seven stroke subjects and in two functional targets of stroke subjects. One healthy subject shows a negative field strength after stimulation with the contralateral conventional configuration in the functional target. All healthy subjects have for the anatomical target a positive field strength for the contralateral conventional configuration, with the 0.06 V/m as the lowest field strength. This implies that the conventional configuration could be a suitable configuration for tDCS in healthy subjects to target the motor hand function area based on the found directions of the field strength.

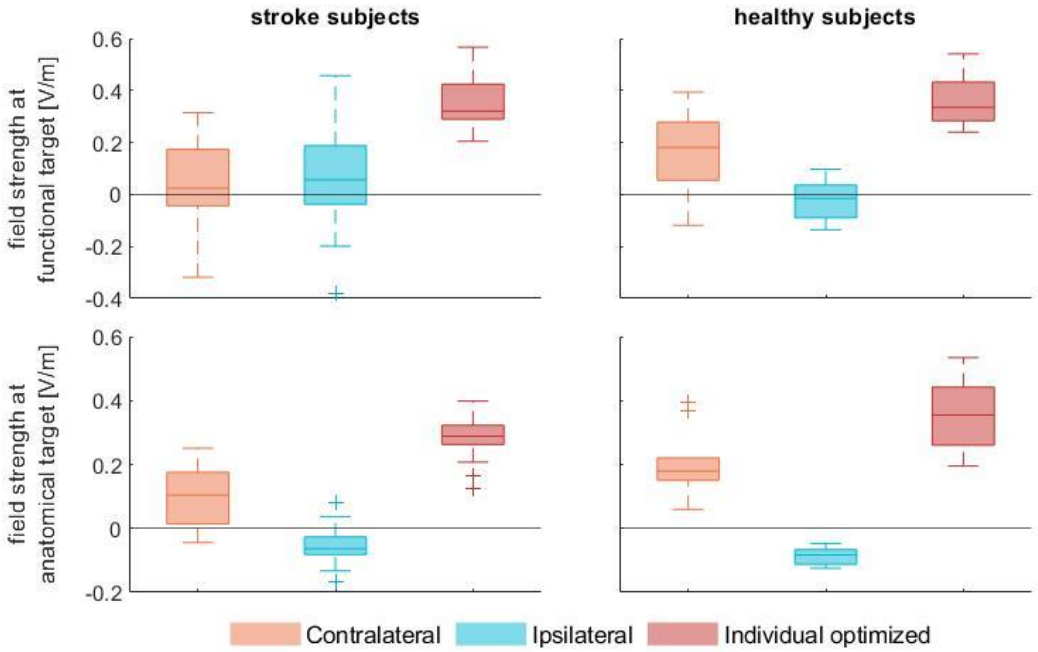

Figure 5. A boxplot of the field strengths per target, configuration and group of subjects in V/m.

3.2.3.2. Comparison of electrode configurations

The used anodes in the optimized 2-electrode tDCS configurations for the anatomical targets are in all stroke subjects and healthy subjects (adjacent to) the contralateral conventional anode. Figure 6 presents an overview of which electrodes are used in the individual optimized 2-electrode configurations. All configurations are corrected for the targeted hemisphere; all targets are considered on the left hemisphere. If we look at the healthy subjects in the anatomical target, seven subjects have C3 as the anode, three C5. This endorses the use of C3 as the anode in the conventional configuration. In the anatomical target of stroke subjects, we see C5 ten times as anode, C3 three times, CP5 and FC5 two times, and FC3 and CP3 once.

For the functional target, the used anode is more varied. For the healthy subjects, the anodes are all (adjacent to) C3, except for one; one anode is placed on the ipsilateral hemisphere (FC2). For the stroke subjects, fifteen anodes are (adjacent to) C3. Of the other six anodes, for are ipsilateral, and one is medial.

The cathodes used in the individual optimized configurations are more different and not similar to the location of the cathode used in conventional configurations (Fp2). The cathodes in the

individual optimized configurations for the anatomical targets are for both subject groups in most cases located on or near the central midline. The locations of the cathodes for the functional target are very divided in both subject groups.

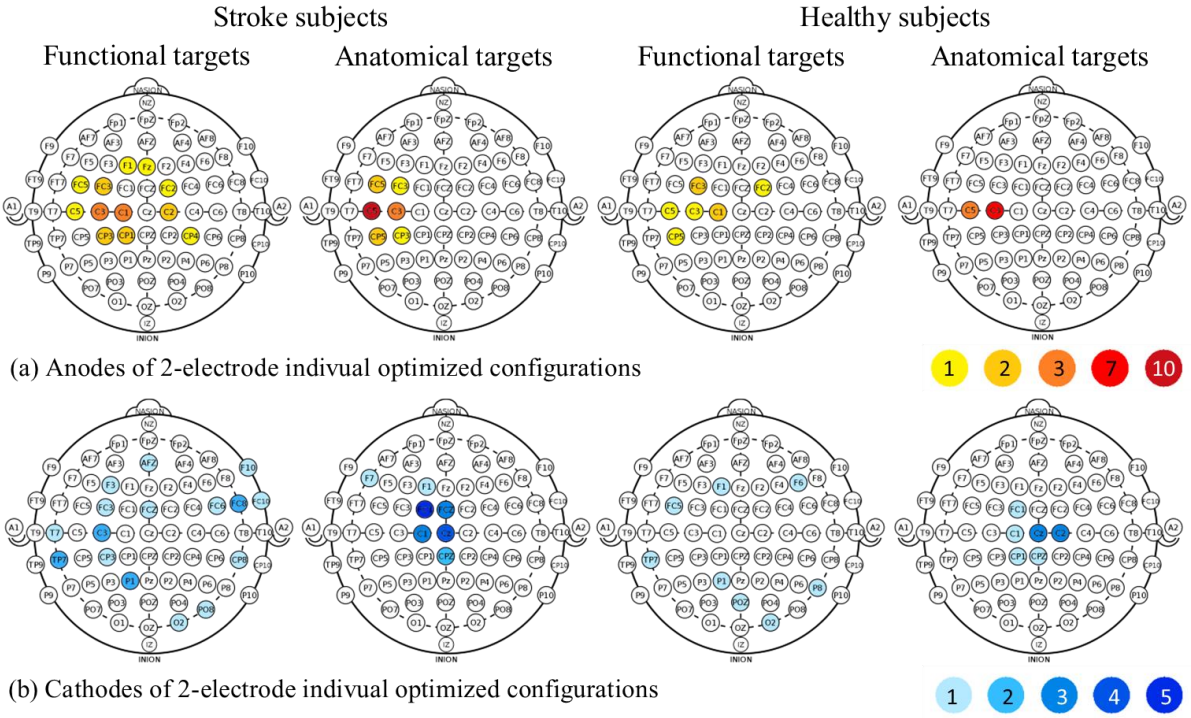

Figure 6. An overview of the electrodes used as anode or cathode in individual optimized 2-electrode configurations, per target and group of subjects. The colours represent the number of times an electrode is used as anode (1, 2, 3, 7 or 10) or cathode (1, 2, 3, 4 or 5) in the individual optimized configurations. All configurations made for stimulating the right hemisphere are mirrored to the left hemisphere for this figure to compare the occurrences more easily. The anode used in conventional stimulation is C3, the cathode is Fp2.

3.2.4. The effect of an increased number of electrode pairs

Figure 7 presents the increase in field strength for both the functional and anatomical targets for multiple electrode pairs: 2, 4, 6 and 8 electrodes. It can be seen that the field strength does not linearly increase when adding an extra pair of electrodes. This non-linearity is as expected since each additional electrode pair in the optimization should result in a smaller contribution to the total field strength compared to the two-electrode optimization. The differences in the mean of the field strength between the stroke and healthy subjects in the functional target are negligible; for the anatomical tDCS target, the difference is a bit larger. For the anatomical targets, the mean of the stroke subjects (2 electrodes 0.28±0.07, 4 electrodes 0.54±0.14, 6 electrodes 0.77±0.20, 8 electrodes 0.99±0.24) is lower than for the healthy subjects (2 electrodes 0.35±0.11, 4 electrodes 0.65±0.20, 6 electrodes 0.90±0.28, 8 electrodes 1.15±0.36).

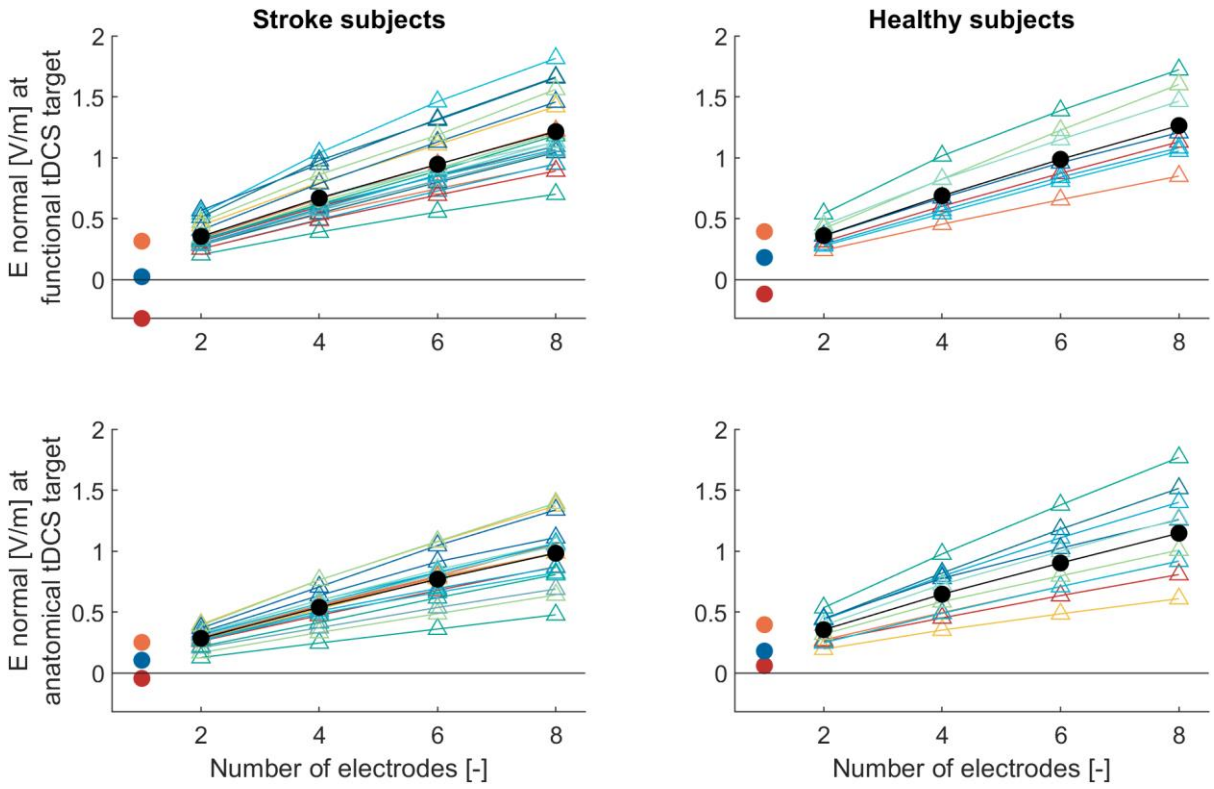

Figure 7. The field strength of E normal at the functional (top) and anatomical (bottom) tDCS target per subject, with different numbers of electrodes. Each line represents a subject, and each triangle an optimization for that subject. The black line with the black dots represents the mean E normal field strength of the individual optimized configurations per number of electrodes. The red, blue, and orange dots represent the contralateral conventional configuration's minimum, median, and maximum field strength. The field strengths of the optimized configurations per subject do not increase linearly with the increase of electrode pairs, which shows the 2-electrode-configuration to be optimal. The subjects for whom a target was not found are excluded from this figure.

4. Discussion

This study evaluated the effect of individual optimized tDCS configurations in chronic stroke patients on simulated field strength compared to conventional tDCS configurations in terms of intensity of field strength. The individual optimized tDCS configurations were optimized to maximally stimulate an individual functional or anatomical target. The functional target is based on EEG, obtained during a functional hand task. The individual optimized configuration for the functional target is built considering the functional and structural reorganization. The anatomical target is based on the location of the hand knob in the motor cortex, determined by individual anatomy in the MRI. The individual optimized configuration for the anatomical target is built considering the structural reorganization.

4.1. Principal findings

4.1.1. Anatomical target

In the first place, we showed that the conventional tDCS configuration for healthy subjects always simulated with a positive, thus stimulating, field strength in the anatomical target. Therefore, the conventional tDCS configuration can be considered suitable to stimulate the anatomical target with a positive field strength in healthy subjects. However, literature shows that inter-individual functional variability. Therefore, it is important to note that even though the conventional configuration is suitable for stimulating the anatomical target, it is not known if this may have any physical effect(Lefebvre et al., 2019).

If we look at the anodes of the 2-electrode individual optimized configurations, we see for seven of the ten healthy subjects the electrode C3 as the anode, and three the adjacent C5. This indicates the anode of conventional configuration to be suitable in healthy subjects. However, after simulating the individual optimized tDCS configurations for this group in the anatomical target, the median field strength is twice as high, which shows the beneficial potential of individual optimized tDCS configurations. The difference in field strength between the conventional and individual optimized configurations is most likely caused by the difference in location of the cathode since the applied currents and the anode are the same, with the exception of the three subjects with the C5 anode, adjacent to C3. The cathode in the conventional configurations is Fp2 on the ipsilateral supraorbital. The cathodes used in the individual optimized configurations are placed on the midline central electrode Cz, or adjacent to Cz. We focused on evaluating the fields strengths in the targets. Herein we did not consider the distribution of the electric field. Literature shows that field strength outside of the target may induce a physical effect(Fischer et al., 2017; Nitsche et al., 2015). Therefore, even though the individual optimized configurations show a higher field strength than the conventional configuration, we can not say that the physical effect will also increase based on these field strengths.

The simulation of the contralateral conventional configuration resulted in the anatomical target of stroke subjects in mixed findings: positive, low and negative field strengths. Two stroke subjects showed a negative field strength in the anatomical target, in simulation of the contralateral conventional configuration. For two other stroke subjects, no anatomical target was found due to the lesion at that location. Since we evaluate and compare field strengths, we cannot include those subjects. However, with the knowledge that the functional target of those subjects was found ipsilateral, we assume the resulting effects of contralateral conventional tDCS for those subjects unpredictable. Furthermore, four of the stroke subjects with a positive field strength in the anatomical target have a low field strength (<0.02 V/m). Previous research showed a positive link between simulated field strength and empirically assessed brain stimulation effects, where the higher the electric field strength at the target, the more likely the brain region's cortical excitability is modulated(Antonenko et al., 2019; Kim et al., 2014). However, currently, there is no known threshold for a stimulated dosage that is sufficient to induce physiological effects in the cortex (Caulfield et al., 2020). Therefore, we can not say anything about the clinical effects of the field strengths we found. However, we can assume that lower field strengths may have a negligible effect.

Thus, the simulated field strengths of the contralateral conventional configurations were in two stroke subjects negative, in four subjects possibly negligible, and for two subjects no anatomical target was found, where the effects of conventional configuration are unpredictable. Therefore, we assume that conventional tDCS configurations are unsuitable for applying on stroke patients, when targeting the anatomical target.

The simulations of the individual optimized configurations result for all stroke subjects in a positive field strength in the anatomical target. This indicates that the stroke subjects are stimulable in the anatomical target.

4.1.2. Functional target

In the previous section, we discussed the consistent field strengths in the anatomical targets of the healthy subjects after simulation of the conventional configuration. These conventional tDCS simulations show less consistent results in the functional target of the healthy subjects: one functional target was stimulated with negative field strength. This subject's total distance between the anatomical and functional target is the largest of all subjects (See Appendix B.), and this functional target is not located on M1. The conventional configuration is designed to target M1; the fact that this functional target is not on M1 may explain this negative field strength. Furthermore, we can not evaluate the conventional configuration in the functional target for two healthy subjects since no functional target was found.

Eight of the functional targets for stroke subjects were located ipsilateral, twelve contralateral, and no functional target was found for one subject. In a clinical setting is often no functional reorganization considered, and a contralateral conventional tDCS configuration would be applied, targeting the contralateral hemisphere. Thus, for eight stroke subjects, the wrong hemisphere would be stimulated with the conventional configuration, considering their ipsilateral functional target. Thus, the functional reorganization in stroke patients may contribute to the mixed findings in previous research with applying conventional tDCS configurations in stroke patients. Therefore, considering functional reorganization to target the functional hemisphere when applying conventional tDCS in stroke patients could be beneficial. However, stimulating these subjects with the conventional configuration targeting the ipsilateral hemisphere does not guarantee a positive or higher field strength compared to the contralateral configuration. Three of these eight stroke subjects with an ipsilateral functional target have a higher field strength for the contralateral conventional configuration than the ipsilateral conventional configuration. More examples of mixed findings in field strength after simulation of the conventional configurations in the functional target in stroke subjects are, e.g., some subjects have a negative, inhibiting or low field strength for simulations of both conventional configurations, or a high field strength after simulation with a configuration that is designed to stimulate the not-targeted hemisphere, and low field strength for the opposite configuration. Herein, we emphasize that six stroke subjects have a negative, inhibitory field strength in the functional target after simulation with contralateral conventional tDCS. The mixed findings in simulated field strength, with in some subjects even inhibitory effects, may explain the mixed findings in clinical results in previous tDCS studies(Laakso et al., 2019; Lefebvre & Liew, 2017; Vliet et al., 2017). With the simulations and evaluations we have done in the functional target, it is clear that applying a conventional tDCS configuration in a chronic stroke patient results in mixed field strengths (positive, negative or around zero). If we compare the field strength of the conventional configurations with the individual optimized configurations, it can be seen that the individual optimized configurations results in more consistent field strengths, where the field strengths are always positive and higher than both conventional configurations. These higher and more consistent field strengths of the individual optimized configurations, compared to conventional configurations, may contribute to a more consistent effect of tDCS on motor rehabilitation in stroke patients.

4.2. Comparison with other studies

In this study we simulated field strengths on subject specific head models with inclusion of the lesion, selected individual optimized tDCS configurations and evaluated these configurations in individual anatomical and functional tDCS targets, with a group of 21 stroke patients. This makes this study the largest modelling study of this type. One study (Johnstone et al., 2021) focused on a similar research:

and modelled a variety of synthetic spherical lesions, with a range of lesion conductivity values, in brain models of two healthy participants. In our study, we focused on (the variety in) subject specific characteristics. Therefore is it an added value to use data of stroke patients, compared to using synthetic brain models with lesions.

There are more studies done on simulation of electric fields explaining mixed findings and inter-individual variability in tDCS on the motor cortex(Antonenko et al., 2019; Laakso et al., 2019). However, our study also evaluated the difference in electric field strength between the conventional and individual optimized configuration. This configuration comparison together with this study's focus on stroke patients and taking into account both structural and functional reorganization, makes that this study can provide new insights in this field of research.

4.3. Limitations and future directions

The results of this study should be considered in the context of the following limitations.

First, to optimally select the individual functional target and select the optimal tDCS figuration, it would be best to have a subject-specific volume conductor model as possible. The volume conductor models in this study were built with general tissue conductivities. However, particularly lesion conductivity is variable between subjects (McCann et al., 2019; Minjoli et al., 2017) since brain lesions can appear as an oedema or in calcified form (Vatta et al., 2001). An error in the applied lesion conductivity may lead to incorrect source localization, thus selecting a functional target located away from the real brain source. Furthermore, the lesion conductivity may influence the optimization of the individual tDCS configurations, i.e. with an incorrect lesion conductivity the "real" target may be stimulated sub-optimally(Vorwerk et al., 2014). Therefore, to be able to experimentally assess the effect of the different tDCS configurations, we would recommend to take individual lesion conductivity into account in building the subject-specific volume conduction models.

Secondly, in this study, we focused on the electric field strength in the target area, while we neglected the electric field distribution. However, since brain regions operate with the interaction of other brain regions: a stimulating or inhibiting field strength in a brain region outside the target may impact the targeted or other brain regions or impact the physiological effect(Fischer et al., 2017). Furthermore, we evaluated the normal E component of the field strength. This component is traditionally considered as the main field strength component causing physiological effects. However, more recent studies questioned this view (Antonenko et al., 2019). Furthermore, it is beyond the scope of this study to examine the efficacy on rehabilitation of motor function in stroke patients of the different tDCS configurations. We showed that individual optimized tDCS can increase and show a more consistent electric field strength in a targeted brain area, compared to conventional tDCS configurations. However, the effectiveness of field strength on rehabilitation of the motor function remains to be assessed in a clinical setting. It would be interesting to not only consider the normal E but also the norm E component of the field strength, in a study where the effectiveness of the field strength are experimentally assessed.

Lastly, the simulations with individual optimized configurations with multiple pairs of electrodes showed promising high field strengths. Future studies have to be done on these configurations and physical effects, which may result in far more effective tDCS in chronic stroke patients.

5. Conclusion

This study aimed to determine if individualized tDCS configurations show less variable stimulation strengths compared to conventional configurations. The individual optimized configurations are optimized to stimulate maximally (i) the anatomical target; in this configuration is the structural reorganization taken into account and (ii) the functional target; in this configuration are the structural and functional reorganization considered.

- All healthy subjects had a positive, stimulating field strength in the anatomical target after simulation of the contralateral conventional tDCS configuration. This indicates the contralateral conventional configuration suitable for stimulating the motor hand knob in healthy subjects.
- We have shown that the conventional tDCS configuration may lead to unpredictable, i.e., stimulating, negligible or even inhibitory stimulation in stroke subjects, when simulating while considering structural or structural and functional reorganization. Therefore, we found that the conventional tDCS configuration targeting is unsuitable to stimulate the anatomical or functional target in stroke patients.
- The problem of the unpredictable field strengths in both the anatomical and functional targets after simulation of conventional configurations can be solved by using individual optimized tDCS configurations. The field strength in stroke subjects in the functional target after simulation with individual optimized configurations (median: 0.32 V/m, range: 0.21 – 0.57 V/m) is higher and always positive (stimulating), and therefore more suitable than conventional stimulation (median: 0.02 V/m, range: -0.32 – 0.32 V/m). The same trend can be seen in the anatomical target for the individual optimized configurations (median: 0.29 V/m, range: 0.13 – 0.40 V/m) and conventional configurations (median: -0.10 V/m, range: -0.04 – 0.25V/m).

In conclusion, this study showed that conventional tDCS configurations result in unpredictable, or even inhibiting, field strengths when stimulating the motor hand area in stroke patients. The simulations may explain the lack of consistent therapeutic effects of conventional tDCS in stroke patients and highlight the need for individual optimized tDCS configurations to stimulate the motor hand area in stroke patients.

References

Antonenko, D., Thielscher, A., Saturnino, G. B., Aydin, S., Ittermann, B., Grittner, U., & Flöel, A. (2019). Towards precise brain stimulation: Is electric field simulation related to neuromodulation? *Brain Stimulation*, *12*(5), 1159–1168. https://doi.org/10.1016/j.brs.2019.03.072

Bell, A. J., & Sejnowski, T. J. (1995). An Information-Maximization Approach to Blind Separation and Blind Deconvolution. *Neural Computation*, *7*(6), 1129–1159. https://doi.org/10.1162/neco.1995.7.6.1129

Caulfield, K. A., Badran, B. W., DeVries, W. H., Summers, P. M., Kofmehl, E., Li, X., Borckardt, J. J., Bikson, M., & George, M. S. (2020). Transcranial electrical stimulation motor threshold can estimate individualized tDCS dosage from reverse-calculation electric- field modeling. *Brain Stimulation*, *13*, 961–969. https://doi.org/10.1016/j.brs.2020.04.007

Das, S., Holland, P., Frens, M. A., & Donchin, O. (2016). Impact of transcranial direct current stimulation (tDCS) on neuronal functions. *Frontiers in Neuroscience*, *10*(NOV), 1–7. https://doi.org/10.3389/fnins.2016.00550

Datta, A., Truong, D., Minhas, P., Parra, L. C., & Bikson, M. (2012). Inter-individual variation during transcranial direct current stimulation and normalization of dose using MRI-derived computational models. *Frontiers in Psychiatry*, *3*(October), 1–8. https://doi.org/10.3389/fpsyt.2012.00091

Delorme, A., & Makeig, S. (2004). EEGLAB: an open source toolbox for analysis of single-trial EEG dynamics including independent component analysis. *Journal of Neuroscience Methods*, *134*(1), 9–21. https://doi.org/10.1016/j.jneumeth.2003.10.009

Delorme, A., Palmer, J., Onton, J., Oostenveld, R., & Makeig, S. (2012). Independent EEG sources are dipolar. *PLoS ONE*, *7*(2). https://doi.org/10.1371/journal.pone.0030135

Dmochowski, J. P., Datta, A., Bikson, M., & Su, Y. (2011). Optimized multi-electrode stimulation increases focality and intensity at target. *Journal of Neural Engineering*, *8*. https://doi.org/10.1088/1741-2560/8/4/046011

Dmochowski, J. P., Datta, A., Huang, Y., Richardson, J. D., Bikson, M., Fridriksson, J., & Parra, L. C. (2013). Targeted transcranial direct current stimulation for rehabilitation after stroke. *NeuroImage*, *75*, 12–19. https://doi.org/https://doi.org/10.1016/j.neuroimage.2013.02.049

Fischer, D. B., Fried, P. J., Ruffini, G., Ripolles, O., Salvador, R., Banus, J., Ketchabaw, W. T., Santarnecchi, E., Pascual-Leone, A., & Fox, M. D. (2017). Multifocal tDCS targeting the resting state motor network increases cortical excitability beyond traditional tDCS targeting unilateral motor cortex. *NeuroImage*, *157*, 34–44. https://doi.org/10.1016/j.neuroimage.2017.05.060

Gavaret, M., Marchi, A., & Lefaucheur, J. (2019). Clinical neurophysiology of stroke. In K. H. Levin & P. Chauvel (Eds.), *Clinical Neurophysiology: Diseases and Disorders* (1st ed., Vol. 161, pp. 109–119). Elsevier B.V. https://doi.org/10.1016/B978-0-444-64142-7.00044-8

Huber, R. (2018). *Finding ROI of the double layers in M1*. Layer FMRI Blog. https://layerfmri.com/2018/03/13/finding-roi-of-the-double-layers-in-m1/

Jaillard, A., Martin, C. D., Garambois, K., François Lebas, J., & Hommel, M. (2005). Vicarious function within the human primary motor cortex? A longitudinal fMRI stroke study. *Brain*, *128*(5), 1122–1138. https://doi.org/10.1093/brain/awh456

Jeukens, F. E. M., Schouten, A., Manoochehri, M., Selles, R. W., Cruijsen, J. Van Der, Oostendorp, T., & Piastra, M. C. (2019). *Inclusion of the lesion of chronic stroke patients into a volume conduction model: Vol. c* [TU Delft].

https://repository.tudelft.nl/islandora/object/uuid:9c8dd410-fed7-402a-97a4-b58ee5bf21e6
Johnstone, A., Zich, C., Evans, C., Lee, J., Ward, N., & Bestmann, S. (2021). The impact of brain lesions on tDCS-induced electric field magnitude. *BioRxiv*. https://doi.org/10.1101/2021.03.19.436124
Kim, J., Kim, D., Hyuk, W., Kim, Y., Kim, K., & Im, C. (2014). Inconsistent outcomes of transcranial direct current stimulation may originate from anatomical differences among individuals : Electric field simulation using individual MRI data. *Neuroscience Letters*, *564*, 6–10. https://doi.org/10.1016/j.neulet.2014.01.054
Laakso, I., Mikkonen, M., Koyama, S., Hirata, A., & Tanaka, S. (2019). Can electric fields explain inter-individual variability in transcranial direct current stimulation of the motor cortex? *Scientific Reports*, *9*(1). https://doi.org/10.1038/s41598-018-37226-x
Langhorne, P., Coupar, F., & Pollock, A. (2009). Motor recovery after stroke: a systematic review. In *The Lancet Neurology* (Vol. 8, Issue 8, pp. 741–754). https://doi.org/10.1016/S1474-4422(09)70150-4
Lefebvre, S., Jann, K., Schmiesing, A., Ito, K., Jog, M., Schweighofer, N., Wang, D. J. J., & Liew, S. L. (2019). Differences in high-definition transcranial direct current stimulation over the motor hotspot versus the premotor cortex on motor network excitability. *Scientific Reports*, *9*(1), 1–15. https://doi.org/10.1038/s41598-019-53985-7
Lefebvre, S., & Liew, S. L. (2017). Anatomical parameters of tDCS to modulate the motor system after stroke: A review. *Frontiers in Neurology*, *8*(FEB). https://doi.org/10.3389/fneur.2017.00029
Makeig, S., Bell, A. J., Jung, T.-P., & Sejnowski, T. J. (1996). Independent component analysis of electroencephalographic data. *Advances in Neural Information Processing Systems*, *8*(August). https://doi.org/10.1109/ICOSP.2002.1180091
McCann, H., Pisano, G., & Beltrachini, L. (2019). Variation in Reported Human Head Tissue Electrical Conductivity Values. *Brain Topography*, *32*(5), 825–858. https://doi.org/10.1007/s10548-019-00710-2
Minjoli, S., Saturnino, G. B., Blicher, J. U., Stagg, C. J., Siebner, H. R., Antunes, A., & Thielscher, A. (2017). The impact of large structural brain changes in chronic stroke patients on the electric field caused by transcranial brain stimulation. *NeuroImage: Clinical*, *15*(April), 106–117. https://doi.org/10.1016/j.nicl.2017.04.014
Nitsche, M. A., & Paulus, W. (2000). Excitability changes induced in the human motor cortex by weak transcranial direct current stimulation. *The Journal of Physiology*, *527 Pt 3*(Pt 3), 633–639. https://doi.org/10.1111/j.1469-7793.2000.t01-1-00633.x
Nitsche, M. A., Polania, R., & Kuo, M. F. (2015). Transcranial Direct Current Stimulation: Modulation of Brain Pathways and Potential Clinical Applications. In I. M. Reti (Ed.), *Brain Stimulation: Methodologies and Interventions* (1st ed., pp. 233–254). John Wiley and Sons Inc. https://doi.org/10.1002/9781118568323.ch13
Oostenveld, R, & Praamstra, P. (2001). The five percent electrode system for high-resolution EEG and ERP measurements. *Clinical Neurophysiology : Official Journal of the International Federation of Clinical Neurophysiology*, *112*(4), 713–719. https://doi.org/10.1016/s1388-2457(00)00527-7
Oostenveld, Robert, Fries, P., Maris, E., & Schoffelen, J.-M. (2011). FieldTrip: Open source software for advanced analysis of MEG, EEG, and invasive electrophysiological data. *Computational Intelligence and Neuroscience*, *2011*, 156869. https://doi.org/10.1155/2011/156869
Pfurtscheller, G., Stancák, A., & Neuper, C. (1996). Event-related synchronization (ERS) in the alpha band — an electrophysiological correlate of cortical idling: A review. *International Journal of Psychophysiology*, *24*(1), 39–46.

https://doi.org/https://doi.org/10.1016/S0167-8760(96)00066-9
Piastra, M. C., Cruijsen, J. Van Der, Piai, V., Jeukens, F. E. M., Manoochehri, M., Schouten, A. C., Selles, R. W., & Oostendorp, T. (2021). ASH : an Automatic pipeline to generate realistic and individualized chronic Stroke volume conduction Head models. *Journal of Neural Engineering*, *18*. https://doi.org/10.1088/1741-2552/abf00b
Pustina, D., Coslett, H. B., Turkeltaub, P. E., Tustison, N., Schwartz, M. F., & Avants, B. (2016). Automated segmentation of chronic stroke lesions using LINDA: Lesion identification with neighborhood data analysis. *Human Brain Mapping*, *37*(4), 1405–1421. https://doi.org/10.1002/hbm.23110
Rich, T. L., & Gillick, B. T. (2019). Electrode placement in transcranial direct current stimulation—how reliable is the determination of C3/C4? *Brain Sciences*, *9*(3), 3–9. https://doi.org/10.3390/brainsci9030069
Rozisky, J. R., Antunes, L. C., Brietzke, A., de Sousa, A. C., & Caumo, W. (2016). Transcranial direct current stimulation and neuroplasticity. In L. Rogers (Ed.), *Transcranial Direct Current Stimulation (tDCS): Emerging Uses, Safety And Neurobiological Effects* (Issue January). Nova Science Publishers, Inc.
Saturnino, G. B., Puonti, O., Nielsen, J. D., Antonenko, D., Madsen, K. H., & Thielscher, A. (2018). *SimNIBS 2.1: A Comprehensive Pipeline for Individualized Electric Field Modelling for Transcranial Brain Stimulation*. https://doi.org/https://doi.org/10.1101/500314
Saturnino, G. B., Siebner, H. R., Thielscher, A., & Madsen, K. H. (2019). Accessibility of cortical regions to focal TES: Dependence on spatial position, safety, and practical constraints. *NeuroImage*, *203*(September), 116183. https://doi.org/10.1016/j.neuroimage.2019.116183
Siegel, J. S., Seitzman, B. A., Ramsey, L. E., Ortega, M., Gordon, E. M., Dosenbach, N. U. F., Petersen, S. E., Shulman, G. L., & Corbetta, M. (2018). Re-emergence of modular brain networks in stroke recovery. *Cortex; a Journal Devoted to the Study of the Nervous System and Behavior*, *101*, 44–59. https://doi.org/10.1016/j.cortex.2017.12.019
Thielscher, A., Antunes, A., & Saturnino, G. B. (2015). Field modeling for transcranial magnetic stimulation: A useful tool to understand the physiological effects of TMS? *37th Annual International Conference of the IEEE Engineering in Medicine and Biology Society (EMBC)*, 222–225. https://doi.org/10.1109/EMBC.2015.7318340
Vatta, F., Bruno, P., & Inchingolo, P. (2001). EEG source localization sensitivity due to brain lesions modeling errors. *2001 Conference Proceedings of the 23rd Annual International Conference of the IEEE Engineering in Medicine and Biology Society*, 913–916. https://doi.org/10.1109/IEMBS.2001.1019093
Vlaar, M. P., Solis-Escalante, T., Dewald, J. P. A., Van Wegen, E. E. H., Schouten, A. C., Kwakkel, G., & Van Der Helm, F. C. T. (2017). Quantification of task-dependent cortical activation evoked by robotic continuous wrist joint manipulation in chronic hemiparetic stroke. *Journal of NeuroEngineering and Rehabilitation*, *14*(1), 1–15. https://doi.org/10.1186/s12984-017-0240-3
Vliet, R. Van Der, Ribbers, G. M., Vandermeeren, Y., Frens, M. A., & Selles, R. W. (2017). BDNF Val66Met but not transcranial direct current stimulation affects motor learning after stroke. *Brain Stimulation*, *10*(5), 882–892. https://doi.org/10.1016/j.brs.2017.07.004
Vorwerk, J., Cho, J., Rampp, S., Hamer, H., Knösche, T. R., & Wolters, C. H. (2014). A guideline for head volume conductor modeling in EEG and MEG. *NeuroImage*, *100*, 590–607. https://doi.org/10.1016/j.neuroimage.2014.06.040

Abbreviations

ANOVA	Analysis of variance
CSF	Cerebral spinal fluid
EEG	Electroencephalogram
eLORETA	exact low-resolution electromagnetic tomography
GM	Grey matter
ICA	Independent component analysis
MRI	Magnetic resonance imaging
MVC	maximum voluntary contraction
SimNIBS	Simulation of Non-invasive brain stimulation
SNR	signal-to-noise ratio
SSR	steady-state response
tDCS	transcranial direct current stimulation
WM	White matter

A. Overview of targets and field strengths per subject

	ID	Hand	functional target								anatomical target						
			Target coordinate				field strengths				Target coordinate			field strengths			
							conventional [V/m]		optimized					conventional [V/m]		optimized	
			C/I	xyz			CC	IC	[V/m]	ano/catho	xyz			CC	IC	[V/m]	ano/catho
stroke subjects	ID01	L	C	30.14	-0.57	32.80	0.183	-0.032	0.296	C2-O1	46.23	18.29	40.41	0.196	-0.063	0.277	C6-FCz
	ID02	R	-	-	-	-	-	-	-	-	-28.1	22.98	19.9	0.174	-0.082	0.268	C5-Cz
	ID03	L	C	49.70	43.98	28.02	0.227	0.067	0.313	C6-F4	45.18	33.45	35.37	0.015	-0.076	0.261	C6-C2
	ID04	R	I	32.20	37.07	29.72	-0.034	-0.199	0.283	Fz-C4	-	-	-	-	-	-	P8-CP3
	ID05	L	I	-12.88	14.51	61.35	0.211	-0.379	0.541	C2-C3	37.8	24.96	43.34	0.179	-0.039	0.324	C6-FCz
	ID06	L	C	23.89	21.79	30.30	0.165	-0.040	0.205	C4-PO7	29.14	23.4	33.76	0.013	-0.073	0.127	FC4-CPz
	ID07	R	I	30.27	9.13	14.42	0.062	0.016	0.252	C2-T8	-38.3	6.27	11.7	0.146	-0.029	0.268	C5-FCz
	ID08	L	C	27.62	31.89	33.32	0.316	0.068	0.568	C2-F9	46.54	25.53	31.18	0.113	-0.027	0.336	CP6-FC2
	ID09	L	C	57.64	15.30	-7.17	-0.038	-0.033	0.323	F2-TP8	45.59	24.52	26.43	0.001	-0.081	0.167	FC6-Cz
	ID10	R	C	-13.38	12.53	15.95	-0.161	0.189	0.296	C2-FC3	-43.8	9.03	9.63	-0.044	-0.102	0.322	C5-C1
	ID11	L	C	40.24	18.02	32.17	0.037	-0.130	0.338	FC4-P2	46.85	27.9	30.41	0.054	-0.045	0.289	C6-FC2
	ID12	L	C	37.16	37.21	42.45	0.002	-0.143	0.444	FC4-P2	45.91	29.87	40.03	-0.024	-0.102	0.399	C6-C2
	ID13	L	I	-24.61	35.66	17.44	-0.075	0.188	0.253	FC5-FC6	-	-	-	-	-	-	-
	ID14	L	I	-21.49	8.58	6.83	-0.048	0.458	0.512	C3-TP8	46.2	22.5	11.37	0.105	-0.026	0.303	C6-FC2
	ID15	R	I	22.11	11.26	30.42	0.011	0.215	0.321	CP2-FT7	-32.7	31.27	37.59	0.177	-0.068	0.267	C3-Cz
	ID16	R	C	-7.50	32.50	35.04	0.118	0.046	0.328	CP1-FCz	-35.1	23.32	18.28	0.013	0.004	0.218	CP5-FC1
	ID17	L	C	30.04	48.81	24.51	-0.102	0.111	0.294	FC1-T8	43.34	27.5	39.66	0.088	-0.133	0.315	C6-Cz
	ID18	R	C	-14.93	-0.04	32.51	-0.318	0.124	0.406	C4-CP3	-29.9	12.45	35.33	0.096	-0.166	0.368	FC5-CPz
	ID19	R	I	22.53	-2.47	13.62	0.008	0.315	0.473	CP4-FT7	-36.8	19.43	29.19	0.232	-0.022	0.390	C3-FC1
	ID20	L	I	-15.81	23.51	4.86	0.050	0.216	0.351	C1-FT10	60.53	44.26	9.32	0.251	0.079	0.301	C4-F8
	ID21	L	C	30.00	24.93	50.26	0.233	0.039	0.285	CP4-AFz	41.87	25.5	48.77	0.152	0.037	0.208	CP4-F2

(see note on next page)

				Functional target							Anatomical target						
				Target coordinate			Field strengths				Target coordinate			Field strengths			
							Conventional [V/m]		optimized					Conventional [V/m]		optimized	
			C/I	xyz			CC	IC	[V/m]	ano/catho	xyz			CC	IC	[V/m]	ano/catho
Healthy subjects	ID22	L	C	-9.26	52.62	30.53	-0.118	0.098	0.241	FC2-FC5	-35.8	23.24	41.99	0.187	-0.090	0.271	C3-Cz
	ID23	L	C	0.00	0.00	0.00	-0.054	0.050	0.157	C6-TP7	-28.1	17.61	53.41	0.167	-0.047	0.196	C3-C2
	ID24	L	C	-24.09	7.53	22.49	0.055	0.067	0.312	C1-TP7	-43.7	13.87	21.1	0.100	-0.070	0.261	C5-Cz
	ID25	L	C	0.00	0.00	0.00	-0.031	-0.067	0.177	I1-Cz	-48.2	16.55	41.86	0.221	-0.121	0.443	C3-CP1
	ID26	L	C	-30.06	0.92	24.95	0.057	0.006	0.277	CP5-F1	-37	0.36	40.48	0.182	-0.076	0.248	C3-C2
	ID27	L	C	-25.28	14.72	14.80	0.288	-0.009	0.542	C1-I2	-35	5.97	23.21	0.370	-0.090	0.535	C3-Cz
	ID28	L	C	-15.24	47.27	50.08	0.271	-0.020	0.291	FC3-F6	-41.6	26.3	49.89	0.151	-0.052	0.437	C5-FC1
	ID29	L	C	-26.93	24.38	24.56	0.201	-0.107	0.359	FC3-POz	-34.3	6.45	34.65	0.396	-0.066	0.448	C3-C2
	ID30	L	C	-39.88	7.33	50.66	0.162	-0.135	0.418	C5-P1	-30.9	11.48	57.02	0.178	-0.112	0.319	C3-CPz
	ID31	L	C	-26.26	16.05	27.46	0.394	-0.071	0.448	C3-P8	-38.9	18.38	44.37	0.060	-0.125	0.392	C5-C1

Note: This table shows the coordinates of the functional and anatomical targets, and the field strengths found at those targets after stimulation of the contralateral and ipsilateral conventional configuration, and the 2-electrode individual optimized configuration. Of the individual optimized configuration is also the used electrodes presented (anode-cathode). ID: subject number, hand indicates the measured hand during EEG (L=left hand, R= right hand). C/I indicates whether the functional target is located contralateral (C) or ipsilateral. CC = contralateral conventional configuration, IC = ipsilateral conventional configuration.

B. Overview of distance between functional and anatomical targets

			Distance between targets [mm]			
Stroke subjects			x	y	z	total
ID01			-16.09	-18.86	-7.61	25.93
ID02			-	-	-	-
ID03			4.52	10.53	-7.35	13.61
ID04			-	-	-	-
ID05			-	-	-	-
ID06			-5.25	-1.61	-3.46	6.49
ID07			-	-	-	-
ID08			-18.92	6.36	2.14	20.08
ID09			12.05	-9.22	-33.60	36.87
ID10			-30.43	3.50	6.32	31.27
ID11			-6.61	-9.88	1.76	12.02
ID12			-8.75	7.34	2.42	11.68
ID13			-	-	-	-
ID14			-	-	-	-
ID15			-	-	-	-
ID16			-27.60	9.18	16.76	33.57
ID17			-13.30	21.31	-15.15	29.33
ID18			-14.96	-12.49	-2.82	19.69
ID19			-	-	-	-
ID20			-	-	-	-
ID21			-11.87	-0.57	1.49	11.97
	median		-12.58	1.46	-0.66	19.88
	min		-30.43	-18.86	-33.60	6.49
	max		12.05	21.31	16.76	36.87
	median	absolute	12.68	9.20	4.89	
	min	absolute	4.52	0.57	1.49	
	max	absolute	30.43	21.31	33.60	
Healthy subjects						
ID22			26.53	29.38	-11.46	41.21
ID23			-	-	-	-
ID24			19.63	-6.34	1.39	20.68
ID25			-	-	-	-
ID26			6.96	0.56	-15.53	17.03
ID27			9.73	8.75	-8.41	15.55
ID28			26.33	20.97	0.19	33.66
ID29			7.37	17.93	-10.09	21.85
ID30			-8.94	-4.15	-6.36	11.73
ID31			12.59	-2.33	-16.91	21.21
	median		11.16	4.65	-9.25	20.94
	min		-8.94	-6.34	-16.91	11.73
	max		26.53	29.38	1.39	41.21
	median	absolute	11.16	7.54	9.25	
	min	absolute	6.96	0.56	0.19	
	max	absolute	26.53	29.38	16.91	

Table B. An overview of distance between functional and anatomical target per subject.

Note: The distances are compensated for the hemisphere, meaning that the positive distance in the x-direction indicates an anatomical target to be medial to the functional target. Furthermore, a positive distance in the y-direction indicates an anatomical target posterior to the functional target, and a positive distance in the x-direction indicates the anatomical target inferior to the functional target.
The distances are missing for the subjects with no anatomical or functional target, or with an ipsilateral functional target.
The median, minimum and maximum distance between the two targets in the x, y and z-direction are given, together with the median, minimum and maximum of the absolute values.

C. MATLAB Masterscript for SimNIBS

Contents

MASTER SCRIPT

this script is to run optimisations and simulations for all subjects, and refers to all different steps and functions.

NEEDED FUNCTIONS TO RUN:

- **leadfield_calculations():** creates leadfield of subjects
- **gifti2mesh_lesion()**: creates gifti mesh for stroke subjects, with relabeled lesion. This is needed for SimNIBS' source code, because gifti by default doesn't have a labeled lesion. note: fieldtrip needed, with cd C:\fieldtrip-20210111 (or change this in this function)
- **gifti2mesh_no_lesion():** healthy subjects don't have a linda-folder, therefore a separate function. (Could have been build in in the other one.)
  note: fieldtrip needed, with cd C:\fieldtrip-20210111 (or change this in this function)
- **tDCS_optimisation()**
- **run_config_optim()**
- **tDCS_optimisation_hk():** same as tDCS_optimisation, but with the anatomical target
- **ROI_with_map_to_surf()**
- **run_config_standard():** runs conventional configurations
- **ROI_with_map_to_surf_standard():** for conventional configurations

Needed functions that are included by default in SimNIBS:

- **mesh_load_fssurf()**
- **mesh_save_gmsh4()**
- **mesh_get_triangle_centers()**

```
% NEEDED FILES / FILES STRUCTURE
%       - 'subject_info.mat' in this folder, with subject IDs, the impaired
%            hand, the dipole target, hand knob (HK) target, and the
%            closest node to the latter two.


clear all; close all; clc

addpath('C:\Users\<USER_NAME>\AppData\Local\SimNIBS\matlab')

pts = 'D:\itDCS2\Data';   %'path_to_subjects';
subjects = {'18801','18802','18803','18804','18805', '18806','18807',...
    '18808','18809','18810','18811','18812','18813','18814','18815',...
    '18816','18817', '18818','18819','18820','18821','19901','19902',...
    '19903','19904','19905','19906','19907','19908','19909','19910'};

load('subject_info.mat');
lesion_info = table2cell(subject_info);
```

0.a Find closest node to target

the found targets are not exactely defined on a node, but SimNIBS recalculates the targets to nodes. For having the same result for the optimisation and stimulation, the closest node is computed here.

```
for i=1:length(subjects)
```

```
    sub = subjects{i};
    hdf5 = sprintf('%s_leadfield_EEG10-10_UI_Jurak_2007.hdf5', sub);
    lf_mesh = mesh_load_hdf5(fullfile(pts, sub, 'leadfield', hdf5));

    target = [];
    for j=1:length(lesion_info)
            if ismember(lesion_info{j,1}, str2num(sub)) %check sub nr
                target = table2array(subject_info(j,3));    % functional target
                HK = table2array(subject_info(j,7));        % anatomical target
            end
    end

    idx = knnsearch(lf_mesh(2).mesh.nodes, target); % index for closest node to
dipole target
    idx_HK = knnsearch(lf_mesh(2).mesh.nodes, HK);  % index for closest node to HK
target
    for j=1:length(lesion_info)
        if ismember(lesion_info{j,1}, str2num(sub))
            subject_info.target_node(j,:) = lf_mesh(2).mesh.nodes(idx,:);
            subject_info.HK_node(j,:) = lf_mesh(2).mesh.nodes(idx_HK,:);
        end
    end
end

save subject_info subject_info
```

0.b Create struct to save results to

```
struct = struct()

for jj=1:length(subjects)
    struct = setfield(struct,{jj},'subject',subjects(jj));
    struct = setfield(struct,{jj},'lesion_side',lesion_info(jj,2));
    struct = setfield(struct,{jj},'target_xyz',lesion_info(jj,3));
    struct = setfield(struct,{jj},'target_hemi',lesion_info(jj,4));
end
```

1. Gifti2mesh; Include lesion in gifti and make it a mesh

With making the headmodel, gifti-files (.gii) are created. These files are surface files and don't include info on the lesion, thus this needs to be changed. Can be done with the function gifti2mesh

```
gifti2mesh_lesion(subjects(1:21), pts);       % for stroke subjects
gifti2mesh_no_lesion(subjects(22:end), pts);  % for healthy subjects
```

2. Get leadfield

```
leadfield_calculations(subjects,pts);
```

3. Optimise, run optimisation & find fieldstrength

this function loads target coordinates with subject_info.mat creates map tDCS_optimisation() - does optimisation run_config_optim() - runs optim config this function creates a folder in the already created pts\sub\optimisation folder: pts\sub\optimisation\sub_config_optim ROI_with_map_to_surf() - finds fieldstrength normal E at target sphere

```
max_elec = [2 4 6 8];
```

```
for i=1:length(max_elec)
    % for functional target
    tDCS_optimisation(subjects, pts, max_elec(i), subject_info)
    run_config_optim(subjects, pts, max_elec(i))
    ALL_OUTPUT = ROI_with_map_to_surf(subjects, pts, max_elec(i), subject_info,
ALL_OUTPUT)
    save ALL_OUTPUT.mat ALL_OUTPUT

    % for anatomical target
    tDCS_optimisation_hk(subjects,pts,max_elec(i),subject_info)  % also includes
the 'run_config_optim'-part
end
```

4. Run standard configurations & find field strength

two standard configurations; for botwh hemispheres. run_config(subjects, cathode, anode, pts);

```
run_config_standard(subjects, 'Fp2', 'C3', pts); %Fp2 is cathode, C3 is anode
run_config_standard(subjects, 'Fp1', 'C4', pts);

struct = ROI_with_map_to_surf_standard(subjects, subject_info, pts, 'Fp2', 'C3',
struct)
struct = ROI_with_map_to_surf_standard(subjects, subject_info, pts, 'Fp1', 'C4',
struct)

save struct.mat struct
```

5. Plot overview mesh of subject with lesion, target, impaired hand

```
for i=1:length(subjects)
    sub = subjects{i};
    target = [];
    for j=1:length(lesion_info)
            if ismember(lesion_info{j,1}, str2num(sub)) % check sub nr to find
target
                target = table2array(subject_info(j,3));
            end
            if ismember(lesion_info{j,1}, str2num(sub)) &
strcmp(lesion_info{j,2},'L') % check sub to find impaired hand
                im = imread('righthand.png'); % load image of hand
                side_lesion = 'Lesion Left';
                im_x = [58 88];
                im_y = [120 90];
            elseif ismember(lesion_info{j,1}, str2num(sub)) &
strcmp(lesion_info{j,2},'R') % check sub to find impaired hand
                im = imread('lefthand.png');
                side_lesion = 'Lesion Right';
                im_x = [-90 -60];
                im_y = [120 90];
            elseif ismember(lesion_info{j,1}, str2num(sub)) &
strcmp(lesion_info{j,2}, 'x')  % for healthy subjects
                side_lesion = 'Healty subject';
                im = imread('peppers.png');
                im_x = [60 90];
                im_y = [120 90];

            end
    end

    optim_config = sprintf('%s_Fp2C3',sub);  % mesh file that is mapped to GM
middle layer (node values not important)
```

```
    file = sprintf('%s_TDCS_1_scalar_central',sub); % name of mesh file
    surf = mesh_load_gmsh4(fullfile(pts,sub, optim_config, 'subject_overlays', [
file '.msh']));  % load mesh file- surface

    r = 5;       % radius of visualization ROI in mm (diameter = 10)
                 % note: target r=2mm. this is larger for visualization
    roi_idx = sqrt(sum(bsxfun(@minus, surf.nodes, target).^2, 2)) <r ; %indices of
nodes in ROI (pythagoras)

    surf.node_data{end+1}.data = int8(roi_idx);     % create new node_data entry to
show ROI on mesh
    surf.node_data{end}.name = 'ROI';               % name for new node_data entry

    m = surf;
    m=mesh_extract_regions(m,'elemtype','tri','region_idx',1011);
    cmap = ([200 200 200 ; 195 49 47])/255;         % colormap
    roi_fig = mesh_show_surface_no_colourbar(surf, 'field_idx', 'ROI',
'scaleLimits', [0 1], 'colormap', cmap );
    hold on
    hp = patch('Faces',m.triangles,'Vertices',m.nodes,'FaceVertexCData',([97 164
180])/255,...
        'FaceColor','flat','EdgeColor','none','FaceAlpha',1);
    material(hp,'dull');
    lighting gouraud
    set(gca,'xtick', [])
    set(gca,'ytick', [])
    set(gcf,'color','w');
    hrot = rotate3d;
    set(hrot,'ActionPostCallback',@(~,~)camlight(get(gca,'UserData'),'headlight'));
    image(im_x,im_y,im);        % Plot the image
    xlim([-92 90]);
    ylim([-70 125]);
    text(-85, -65, side_lesion)
    box on
    hold off

    fig_name = sprintf('%s_roi_fig',sub);
    saveas(roi_fig,fullfile(pts, sub, [fig_name '.png']));
end
```

Published with MATLAB® R2020a

D. MATLAB functions for master script

Leadfield_calculations

```
function leadfield_calculations(subjects,pts)
% Example of a SimNIBS tDCS leadfield
% Copyright (C) 2019 Guilherme B Saturnino
% adjusted by Renée Dooren 2020

% automatically finds csv file with EEG electrode positions
% check documentation;
https://simnibs.github.io/simnibs/build/html/documentation/sim_struct/tdcsleadfi
eld.html

tdcs_lf = sim_struct('TDCSLEADFIELD');
tdcs_lf.electrode.thickness = 3;    % 3mm thickness -(default shapes; 1x1cm
round electrode with 4mm thickness)
tdcs_lf.map_to_surf = true;         % map to middle of GM, necessary to be able
to find node_data normal E
tdcs_lf.cond(11).value = 1.6540;    % same value as CSF
tdcs_lf.cond(11).name = 'Lesion';
tdcs_lf.cond(11).type = 'COND';

for i = 1:length(subjects)
    sub = subjects{i};
    tdcs_lf.fnamehead = fullfile(pts, sub, [sub '.msh'] );  % Head mesh
    tdcs_lf.pathfem = fullfile(pts, sub, 'leadfield');      % Output directory
%     tdcs_lf.tissues = [] % Tissues numbers of where to record the electric
field, in addition to map_to_surf. Mixing surfaces and volumes is not allowed.
    % note dat 1006 is default, and in how we altered the original script,
    % 1011 is also included.

    % Uncomment to use the pardiso solver
    %tdcs_lf.solver_options = 'pardiso';
    % This solver is much faster than the default. However, it requires much
more
    % memory (~12 GB)
    run_simnibs(tdcs_lf)
end
end
```

Gifti2mesh_lesion

```
function gifti2mesh_lesion(subjects, pts)
%%%%%%%%%%%%%%%%%%%%%%%%%%%%%%%%%%%%%%%%%%%%%%%%%%%%%%%%%%%%%%%%%%%%%%%%%%%%%%%
% clear all; close all;
cd C:\Users\<USERNAME>\SimNIBS-3.2\matlab
load('lesion_side.mat');
lesion_info = table2cell(lesion_side);

for i=1:length(subjects)
    sub = subjects{i};


    subject = str2num(sub);


    surf_gif = mesh_load_fssurf(fullfile(pts,sub, ['m2m_' sub]));  % load
surfacemesh from GIFTI files (both hemispheres)
    lh_surf_gif = mesh_load_fssurf(fullfile(pts,sub, ['m2m_' sub]), 'hemi', 'lh');
% load left hemisphere from gifti
    rh_surf_gif = mesh_load_fssurf(fullfile(pts,sub, ['m2m_' sub]), 'hemi', 'rh');
% load right hemisphere from gifti
    % mesh_show_surface(surf_gif);
    cd C:\fieldtrip-20210111
```

```
    ft_defaults  % load fieldtrip

    %load lesion mask segmented by LINDA
    filename = [];
    filename = fullfile(pts, sub, 'linda\Prediction3_native.nii.gz');
    gunzip(filename);
    lesion_mask = ft_read_mri(filename(1:end-3));

%%%%%%%%%%%%%%%%%%%%%%%%%%%%%%%%%%%%%%%%%%%%%%%%%%%%%%%%%%%%%%%%%%%%%%%%%%%%%%%
% FIND COORDINATES OF LESION MASK

    [r,c,v] = ind2sub(size(lesion_mask.anatomy),find(lesion_mask.anatomy == 1)); %
get the indices of lesion voxels
    lesion_vox = [r c v];                   %voxels of the lesion
    lesion_coord = lesion_mask.transform*[lesion_vox ones(length(lesion_vox),1)]';
% from voxel indices to head-coordinates
    lesion_coordinates = lesion_coord(1:3,:)';

    if isempty(lesion_coord) % if lesion is not found by LINDA, directly save the
meshes without adding lesion labels
        lesion_hm = surf_gif;
        lh_lesion_hm = lh_surf_gif;
        rh_lesion_hm = rh_surf_gif;
        cd C:\Users\renee\SimNIBS-3.2\matlab
        mesh_save_gmsh4(lesion_hm, fullfile(pts,sub, ['m2m_' sub],
'mesh_midgm_with_lesion'))
        mesh_save_gmsh4(lh_lesion_hm, fullfile(pts,sub,['m2m_' sub],
'lh_midgm_with_lesion'))
        mesh_save_gmsh4(rh_lesion_hm, fullfile(pts,sub,['m2m_' sub],
'rh_midgm_with_lesion'))
    else

         %%%%%%%%%%%%%%%%%%%%%%%%%%%%%%%%%%%%%%%%%%%%%%%%%%%%%%%%%%%%%%%%%%%%%%%%%%%%%%%
         % FIND CENTERS OF ELEMENTS

        cd C:\Users\<USERNAME>\SimNIBS-3.2\matlab
        centers_triangles = mesh_get_triangle_centers(surf_gif); % Centers

        %%%%%%%%%%%%%%%%%%%%%%%%%%%%%%%%%%%%%%%%%%%%%%%%%%%%%%%%%%%%%%%%%%%%%%%%%%%%%%%
         % FILTER ON DISTANCE BETWEEN VOXEL AND ELEMENENT (triangles)

        [idx_vox_tri,D] = knnsearch(lesion_coordinates,centers_triangles); %index
voxel closest to element, D = distance between element and closest voxel
        A_tri = [idx_vox_tri, D];
        A_tri(:,3) = 1:size(A_tri,1); %element index
        A_tri(A_tri(:,2)>2,:) = []; % Only keep indeces with a distance shorter
than 2mm (for computing time)
        %%%%%%%%%%%%%%%%%%%%%%%%%%%%%%%%%%%%%%%%%%%%%%%%%%%%%%%%%%%%%%%%%%%%%%%%%%%%%%%
         % FIND ELEMENTS WITHIN LESION VOXELS
        wx=1; wy=1; wz=1;


        % Triangles
        K_tri = [];
            for i = 1:length(A_tri)
                if centers_triangles((A_tri(i,3)),1) >
lesion_coordinates(A_tri(i,1),1) - wx/2 && centers_triangles((A_tri(i,3)),1) <
lesion_coordinates(A_tri(i,1),1) + wx/2 && ...
                        centers_triangles((A_tri(i,3)),2) >
lesion_coordinates(A_tri(i,1),2) - wy/2 && centers_triangles((A_tri(i,3)),2) <
lesion_coordinates(A_tri(i,1),2) + wy/2 && ...
                        centers_triangles((A_tri(i,3)),3) >
lesion_coordinates(A_tri(i,1),3) - wz/2 && centers_triangles((A_tri(i,3)),3) <
lesion_coordinates(A_tri(i,1),3) + wz/2
                    K_tri(i,1) = A_tri(i,3); % gives indices of lesion elements
                end
            end
        K_tri(K_tri==0) = []; % delete zeros
```

```
        idx_lesion_tri = K_tri;
        %%%%%%%%%%%%%%%%%%%%%%%%%%%%%%%%%%%%%%%%%%%%%%%%%%%%%%%%%%%%%%%%%%%%%%%%
         % REPLACE CORRESPONDING LABELS WITH LESION LABEL (11)
        lesion_hm = surf_gif; lh_lesion_hm = lh_surf_gif; rh_lesion_hm =
rh_surf_gif;

        lesion_hm.triangle_regions(idx_lesion_tri)=1011;

        for i=1:length(lesion_info)
            if ismember(lesion_info{i,1}, str2num(sub)) &
strcmp(lesion_info{i,2},'L') %check sub nr and lesion side
                lh_lesion_hm.triangle_regions(idx_lesion_tri)=1011;

            elseif ismember(lesion_info{i,1}, str2num(sub)) &
strcmp(lesion_info{i,2},'R') %check sub nr and lesion side
                centers_triangles_rh = mesh_get_triangle_centers(rh_surf_gif);
%Centers triangles

                % Filter on distance between voxel and element
                [idx_vox_tri_rh,D_rh] =
knnsearch(lesion_coordinates,centers_triangles_rh); %index voxel closest to
element, D = distance between element and closest voxel
                A_tri_rh = [idx_vox_tri_rh, D_rh];
                A_tri_rh(:,3) = 1:size(A_tri_rh,1); %element index
                A_tri_rh(A_tri_rh(:,2)>2,:) = []; % Only keep indeces with a
distance shorter than 2mm (for computing time)

%%%%%%%%%%%%%%%%%%%%%%%%%%%%%%%%%%%%%%%%%%%%%%%%%%%%%%%%%%%%%%%%%%%%%%%%
% FIND ELEMENTS WITHIN LESION VOXELS
                wx=1; wy=1; wz=1;


                % Triangles
                K_tri_rh = [];
                    for i = 1:length(A_tri_rh)
                        if centers_triangles_rh((A_tri_rh(i,3)),1) >
lesion_coordinates(A_tri_rh(i,1),1) - wx/2 &&
centers_triangles_rh((A_tri_rh(i,3)),1) < lesion_coordinates(A_tri_rh(i,1),1) +
wx/2 && ...
                                centers_triangles_rh((A_tri_rh(i,3)),2) >
lesion_coordinates(A_tri_rh(i,1),2) - wy/2 &&
centers_triangles_rh((A_tri_rh(i,3)),2) < lesion_coordinates(A_tri_rh(i,1),2) +
wy/2 && ...
                                centers_triangles_rh((A_tri_rh(i,3)),3) >
lesion_coordinates(A_tri_rh(i,1),3) - wz/2 &&
centers_triangles_rh((A_tri_rh(i,3)),3) < lesion_coordinates(A_tri_rh(i,1),3) +
wz/2
                            K_tri_rh(i,1) = A_tri_rh(i,3); % gives indices of
lesion elements
                        end
                    end
                K_tri_rh(K_tri_rh==0) = [];
                idx_lesion_tri_rh = K_tri_rh;
                rh_lesion_hm.triangle_regions(idx_lesion_tri_rh)=1011;
            end
        end

%%%%%%%%%%%%%%%%%%%%%%%%%%%%%%%%%%%%%%%%%%%%%%%%%%%%%%%%%%%%%%%%%%%%%%%%
% SAVE MESHES
        mesh_save_gmsh4(lesion_hm, fullfile(pts,sub, ['m2m_' sub],
'mesh_midgm_with_lesion'))
        mesh_save_gmsh4(lh_lesion_hm, fullfile(pts,sub,['m2m_' sub],
'lh_midgm_with_lesion'))
        mesh_save_gmsh4(rh_lesion_hm, fullfile(pts,sub,['m2m_' sub],
'rh_midgm_with_lesion'))
    end
end
```

Gifti2mesh_no_lesion

```
function gifti2mesh_no_lesion(subjects, pts)
%%%%%%%%%%%%%%%%%%%%%%%%%%%%%%%%%%%%%%%%%%%%%%%%%%%%%%%%%%%%%%%%%%%%%%%%%%%%%%%
% clear all; close all;
cd C:\Users\<USERNAME>\SimNIBS-3.2\matlab
load('lesion_side.mat');
lesion_info = table2cell(lesion_side);

for i=1:length(subjects)
    sub = subjects{i}; % '18806'; % subject ID
    subject = str2num(sub);
    surf_gif = mesh_load_fssurf(fullfile(pts,sub, ['m2m_' sub]));  % load
surfacemesh from GIFTI files (both hemispheres)
    lh_surf_gif = mesh_load_fssurf(fullfile(pts,sub, ['m2m_' sub]), 'hemi', 'lh');
% load left hemisphere from gifti
    rh_surf_gif = mesh_load_fssurf(fullfile(pts,sub, ['m2m_' sub]), 'hemi', 'rh');
% load right hemisphere from gifti
    % mesh_show_surface(surf_gif);

%% REPLACE CORRESPONDING LABELS WITH LESION LABEL (11)

    lesion_hm = surf_gif;


    lh_lesion_hm = lh_surf_gif;


    rh_lesion_hm = rh_surf_gif;

%% SAVE MESHES
% note: meshes are saved as …with_lesion; note that input data for this script, are
% healthy subjects. Thus this file is suboptimal.

    mesh_save_gmsh4(lesion_hm, fullfile(pts,sub, ['m2m_' sub],
'mesh_midgm_with_lesion'))
    mesh_save_gmsh4(lh_lesion_hm, fullfile(pts,sub,['m2m_' sub],
'lh_midgm_with_lesion'))
    mesh_save_gmsh4(rh_lesion_hm, fullfile(pts,sub,['m2m_' sub],
'rh_midgm_with_lesion'))
    % %
end
```

tDCS_optimisation

```
function tDCS_optimisation(subjects,pts,max_elec, subject_info)

% Initialize structure
opt = opt_struct('TDCSoptimize');

lesion_info = table2cell(subject_info);

for i = 1:length(subjects)
    sub = subjects{i};
    crd = [];
    for j=1:length(lesion_info)
            if ismember(lesion_info{j,1}, str2num(sub)) %check sub nr
                crd = table2array(subject_info(j,6));
            end
    end

    file = sprintf('%s_leadfield_EEG10-10_UI_Jurak_2007',sub);
    opt.leadfield_hdf = fullfile(pts, sub, 'leadfield', [file '.hdf5']); % Select
the leadfield file
```

```
    optim = sprintf('opt_%del',max_elec);          % foldername with optimisation
for target with max nr of electrodes
    optfile = sprintf('%s_opt_%del', sub, max_elec);
    opt.name = fullfile(pts, sub, optim, optfile); % Select a name for the
optimization

    opt.target.directions = 'normal';              % target normal E

    opt.max_total_current = max_elec * 1e-3;       % Select a maximum total current
(in A) - if this is larger than max_elec*1e-3, SimNIBS gives incorrect results
    opt.max_individual_current = 2e-3;             % Select a maximum current at
each electrodes (in A)
    opt.max_active_electrodes = max_elec;          % Select a maximum number of
active electrodes (optional)

    % Define optimization target
    opt.target.positions = crd; % position of target, in subjectspace
    opt.target.radius = 2;      % radius around coordinates including in target in
mm

    opt.target.intensity = 10;  % Intensity of the electric field (in V/m)
    opt.open_in_gmsh = 0;       % do not open GMSH

    run_simnibs(opt);           % Run optimisation
end

%%%%%%%%%%%%%%%%%%%%%%%%%%%%%%%%%%%%%%%%%%%%%%%%%%%%%%%%%%%%%%%%%%%%%%%%%%%%%%%
%% EXTRACT RESULTS

for i = 1:length(subjects)
    sub = subjects{i};
    optim = sprintf('opt_%del',max_elec);              % foldername with
optimisation for target with max nr of electrodes
    optfile = sprintf('%s_opt_%del', sub, max_elec);
           % foldername with optimisation for target on one hemisphere (hem)
    optim_config_result = readtable(fullfile(pts, sub, optim, [optfile '.csv']));
    optim_config_result(optim_config_result.Var2 == 0,:) = [] ; % remove all
passive electrodes
    writetable(optim_config_result,fullfile(pts, sub, optim, 'optim_config.txt'));
end
end
```

Published with MATLAB® R2020a

run_config_optim

```
function run_config_optim(subjects, pts, max_elec)
%applying tDCS configurations on given subjects
% needs pwd/subject/subject.msh and optim config
% creates folder subject/subject_catano with files:
%   subject_TDCS_1_scalar
%   subject_TDCS_1_el_currents

s = sim_struct('SESSION');              % Initialization of session
s.map_to_surf = true;

s.poslist{1} = sim_struct('TDCSLIST');  % initialize a tDCS simulation
s.poslist{1}.cond(11).type = 'COND';
s.poslist{1}.cond(11).value = 1.6540;   % conductivity lesion
s.poslist{1}.cond(11).name = 'Lesion';
s.poslist{1}.cond(11).descrip = 'Lesion tissue, same value assumed as CSF';

for i = 1:length(subjects)
    sub = subjects{i};
```

```
    optimisation_name = sprintf('opt_%del',max_elec);% foldername with Optimisation
for target on one hemisphere (hem)
    optim_elec = readtable(fullfile(pts, sub, optimisation_name,
'optim_config.txt'));
    currents = table2array(optim_elec(:,2))';
    centres = (table2array(optim_elec(:,1))');
    s.poslist{1}.currents = [currents];  % set currents [Ampere], must sum zero

    for k=1:length(currents)
        s.poslist{1}.electrode(k).channelnr = k;
        s.poslist{1}.electrode(k).centre = char(centres(k)); % electrode position
        s.poslist{1}.electrode(k).dimensions = [10 10]; % electrode dimension [mm]
        s.poslist{1}.electrode(k).shape = 'ellipse';    % rectangular shape
        s.poslist{1}.electrode(k).thickness = 3;        % 3mm thickness
    end

    s.fnamehead = fullfile(pts, sub, [sub '.msh']);     %used head mesh for
applying tdcs
    sub_config_optim = sprintf('%s_config_optim',sub);  % name for folder to save
config
    s.pathfem = fullfile(pts, sub, optimisation_name, sub_config_optim); % Output
directory
    run_simnibs(s);
end
end
```

tDCS_optimisation_hk

```
function tDCS_optimisation_hk(subjects,pts,max_elec,subject_info)
% This script is used to optimize tDCS configurations for all subjects
% based on the closests node to the contralateral hand knob target

% Initialize structure

opt = opt_struct('TDCSoptimize');
lesion_info = table2cell(subject_info);

for i = 1:length(subjects)
    sub = subjects{i};
    crd = [];

    for j=1:length(lesion_info)
        if ismember(subject_info{j,1}, str2num(sub))    %check sub nr
            crd = subject_info.HK_node(j,:);            % target closests node
        end
    end

    file = sprintf('%s_leadfield_EEG10-10_UI_Jurak_2007',sub);
    opt.leadfield_hdf = fullfile(pts, sub, 'leadfield', [file '.hdf5']); % Select
the leadfield file
    optim = sprintf('opt_%del_HK',max_elec);              % foldername with
optimisation for target with max nr of electrodes
    optfile = sprintf('%s_opt_max%del', sub, max_elec);
    opt.name = fullfile(pts, sub, optim, optfile);  % Select a name for the
optimization

    opt.target.directions = 'normal';   % target normal E

    opt.max_total_current = max_elec * 1e-3;      % Select a maximum total current
(in A)
    opt.max_individual_current = 2e-3;  % Select a maximum current at each
electrodes (in A)
```

```
    opt.max_active_electrodes = max_elec;      % Select a maximum number of active
electrodes (optional)

    % Define optimization target
    opt.target.positions = crd; % position of target, in subjectspace
    opt.target.radius = 2;      % radius aroung coordinates including in target in
mm (we want a sphere around target with 1cm diameter

    opt.target.intensity = 10;  % Intensity of the electric field (in V/m)
    opt.open_in_gmsh = 0;       % do not open GMSH

    run_simnibs(opt);           % Run optimisation
end

%%%%%%%%%%%%%%%%%%%%%%%%%%%%%%%%%%%%%%%%%%%%%%%%%%%%%%%%%%%%%%%%%%%%%%%%%%%%%%%
%% EXTRACT RESULTS

for i = 1:length(subjects)
    sub = subjects{i};
    optim = sprintf('opt_%del_HK',max_elec);    % foldername with optimisation for
target with max nr of electrodes
    optfile = sprintf('%s_opt_max%del', sub, max_elec);
       % foldername with optimisation for target on one hemisphere (hem)
    optim_config_result = readtable(fullfile(pts, sub, optim, [optfile '.csv']));
    optim_config_result(optim_config_result.Var2 == 0,:) = []  % remove all passive
electrodes
    writetable(optim_config_result,fullfile(pts, sub, optim, 'optim_config.txt'));
end

%%%%%%%%%%%%%%%%%%%%%%%%%%%%%%%%%%%%%%%%%%%%%%%%%%%%%%%%%%%%%%%%%%%%%%%%%%%%%%%
%% RUN config_optim PART

s = sim_struct('SESSION');      % Initialization of session
s.map_to_surf = true;

s.poslist{1} = sim_struct('TDCSLIST');  % initialize a tDCS simulation
s.poslist{1}.cond(11).type = 'COND';
s.poslist{1}.cond(11).value = 1.6540;   % conductivity lesion
s.poslist{1}.cond(11).name = 'Lesion';
s.poslist{1}.cond(11).descrip = 'Lesion tissue, same value assumed as CSF';

for i = 1:length(subjects)
    sub = subjects{i};

    optimisation_name = sprintf('opt_%del_HK',max_elec);    % foldername with
optimisation for target on one hemisphere (hem)
    optim_elec = readtable(fullfile(pts, sub, optimisation_name,
'optim_config.txt'));
    currents = table2array(optim_elec(:,2))';
    centres = (table2array(optim_elec(:,1))')
    s.poslist{1}.currents = [currents];  % set currents [Ampere], must sum zero

    for k=1:length(currents)
        s.poslist{1}.electrode(k).channelnr = k;
        s.poslist{1}.electrode(k).centre = char(centres(k));        % electrode
position
        s.poslist{1}.electrode(k).dimensions = [10 10]; % electrode dimension [mm]
        s.poslist{1}.electrode(k).shape = 'ellipse';    % rectangular shape
        s.poslist{1}.electrode(k).thickness = 3;        % 3mm thickness
    end

    s.fnamehead = fullfile(pts, sub, [sub '.msh']);   %used head mesh for applying
tdcs
    sub_config_optim = sprintf('%s_config_optim',sub); % name for folder to save
config
    s.pathfem = fullfile(pts, sub, optimisation_name, sub_config_optim); % Output
directory
    run_simnibs(s);
```

```
end
end
```

Published with MATLAB® R2020a

ROI_with_map_to_surf

```
function [struct]= ROI_with_map_to_surf(subjects, pts, max_elec, subject_info,
struct)

%% Calculates E_norm and/or E_normal in a spherical ROI on mesh

lesion_info = table2cell(subject_info);

for ii=1:length(subjects)
    sub = subjects{ii}
    config = sprintf('%s_config_optim', sub);
    optim = sprintf('opt_%del',max_elec);              % foldername with
optimisation for target with max nr of electrodes

    target = [];
    for j=1:length(lesion_info)
            if ismember(lesion_info{j,1}, str2num(sub)) %check sub nr
%               target = table2array(subject_info(j,6)); % closest node to target
                target = subject_info.target_node(j,:); % closest node to target
            end
    end

    file = sprintf('%s_TDCS_1_scalar_central',sub); % name of mesh file
    surf = mesh_load_gmsh4(fullfile(pts,sub, optim, config, 'subject_overlays', [
file '.msh']));  % load mesh file- surface

    r = 2; % radius of ROI in mm
    roi_idx = sqrt(sum(bsxfun(@minus, surf.nodes, target).^2, 2)) <r ; %indices of
nodes in ROI (pythagoras)

    surf.node_data{end+1}.data = int8(roi_idx);     % create new node_data entry to
show ROI on mesh
    surf.node_data{end}.name = 'ROI';               % name for new node_data entry

    % get field of interest: E_norm
    field_name_normE = 'E_norm';
    field_idx_normE = get_field_idx(surf, field_name_normE, 'node');
    field_normE = surf.node_data{field_idx_normE};

    % get field of interest: E_normal
    field_name_normalE = 'E_normal';
    field_idx_normalE = get_field_idx(surf, field_name_normalE, 'node');
    field_normalE = surf.node_data{field_idx_normalE};

    nodes_areas = mesh_get_node_areas(surf);        % calculate node areas, for
averaging field in ROI

    % Calculate a weighted average of field of interest on ROI
    avg_field_roi_normE = sum(field_normE.data(roi_idx) .*
nodes_areas(roi_idx))/sum(nodes_areas(roi_idx));
    avg_field_roi_normalE = sum(field_normalE.data(roi_idx) .*
nodes_areas(roi_idx))/sum(nodes_areas(roi_idx));

    struct = setfield(struct, {ii}, optim, avg_field_roi_normalE)

    txt = sprintf('%s_electric_field_ROI.txt',sub);% name textfile to print results
    path = fullfile(pts, sub, optim, config, 'subject_overlays', txt);

    optim_elec = readtable(fullfile(pts, sub, optim, 'optim_config.txt'));
```

```
    currents = table2array(optim_elec(:,2))';
    centres = (table2array(optim_elec(:,1))')

    fid = fopen(path,'wt');      % file ID, where to file the printed text
    fprintf(fid, 'Subject: %s - The normE and normalE at ROI\n\n', sub);
    fprintf(fid, 'ROI is a sphere with %g mm radius at coordinates [ %g, %g,
%g]\n', r, target(1), target(2), target(3));
    fprintf(fid, 'mean %s in ROI: %f V/m\n', field_name_normE,
avg_field_roi_normE);
    fprintf(fid, 'mean %s in ROI: %f V/m\n', field_name_normalE,
avg_field_roi_normalE);

end
end
```

Run_config_standard

```
function run_config_standard(subjects, cat, ano, pts)
%applying tDCS configurations on given subjects
% needs pwd/subject/subject.msh
% creates folder subject/subject_catano_ddmmm with files:
%   subject_TDCS_1_scalar
%   subject_TDCS_1_el_currents

% If you want to use more than 2 electrodes, check following link:
%
https://simnibs.github.io/simnibs/build/html/documentation/sim_struct/electrode.htm
l#electrode-struct-doc

% Renée Dooren 20 nov 2020
s = sim_struct('SESSION');                  % Initialization of session
% s.map_to_fsavg = true; %Transform simulation results to FSAverage space
s.map_to_surf = true;

s.poslist{1} = sim_struct('TDCSLIST');     % initialize a tDCS simulation
s.poslist{1}.cond(11).type = 'COND';
s.poslist{1}.cond(11).value = 1.6540;
s.poslist{1}.cond(11).name = 'Lesion';
s.poslist{1}.cond(11).descrip = 'Lesion tissue, same value assumed as CSF';

s.poslist{1}.currents = [-2e-3, 2e-3];     % set currents [Ampere], must sum zero

s.poslist{1}.electrode(1).channelnr = 1;        % Connect electrode to first
channel (-1e-3 A, cathode)
s.poslist{1}.electrode(1).dimensions = [10 10]; % electrode dimension [mm]
s.poslist{1}.electrode(1).shape = 'ellipse';    % rectangular shape
s.poslist{1}.electrode(1).thickness = 3;        % 3mm thickness
s.poslist{1}.electrode(1).centre = cat;         % electrode position
s.poslist{1}.electrode(2).channelnr = 2;        % Connect electrode to second
channel
s.poslist{1}.electrode(2).dimensions = [10 10]; % electrode diameter/dimension [mm]
s.poslist{1}.electrode(2).shape = 'ellipse';    % electrode shape
s.poslist{1}.electrode(2).thickness = 3;        % 5mm thickness
s.poslist{1}.electrode(2).centre = ano;         % electrode position

for i = 1:length(subjects)
    sub = subjects{i};
    s.fnamehead = fullfile(pts,sub, [sub '.msh']);%used head mesh for applying tDCS
    sub_CatAno = sprintf('%s_%s%s',sub, cat, ano); % name for folder to save config
    s.pathfem = fullfile(pts, sub, sub_CatAno);  % Output directory
    run_simnibs(s);
end

end
```

ROI_with_map_to_surf_standard

```
function [struct] = ROI_with_map_to_surf_standard(subjects, lesion_side, pts, cat,
ano, struct)
% Calculates E_norm and/or E_normal in a spherical ROI on mesh
config = sprintf('%s%s_spyder',cat,ano);
lesion_info = table2cell(lesion_side);

for ii=1:length(subjects)
    sub = subjects{ii};
    target = [];
    for j=1:length(lesion_info)
        if ismember(lesion_info{j,1}, str2num(sub)) %check sub nr
%             target = table2array(lesion_side(j,3));
            target = table2array(lesion_side(j,10));
        end
    end

    std_config = sprintf('%s_%s%s',sub, cat, ano);  % name of configuration
    file = sprintf('%s_TDCS_1_scalar_central',sub); % name of mesh file
    surf = mesh_load_gmsh4(fullfile(pts,sub, std_config, 'subject_overlays', [ file
'.msh']));  % load mesh file- surface
    r = 2; % radius of ROI in mm (diameter = 10)
    roi_idx = sqrt(sum(bsxfun(@minus, surf.nodes, target).^2, 2)) <r ; %indices of
nodes in ROI (pythagoras)
    surf.node_data{end+1}.data = int8(roi_idx);     % create new node_data entry to
show ROI on mesh
    surf.node_data{end}.name = 'ROI';               % name for new node_data entry

    % get field of interest: E_norm
    field_name_normE = 'E_norm';
    field_idx_normE = get_field_idx(surf, field_name_normE, 'node');
    field_normE = surf.node_data{field_idx_normE};

    % get field of interest: E_normal
    field_name_normalE = 'E_normal';
    field_idx_normalE = get_field_idx(surf, field_name_normalE, 'node');
    field_normalE = surf.node_data{field_idx_normalE};

    nodes_areas = mesh_get_node_areas(surf);        % calculate node areas, for
averaging field in ROI

    % Calculate a weighted average of field of interest on ROI
    avg_field_roi_normE = sum(field_normE.data(roi_idx) .*
nodes_areas(roi_idx))/sum(nodes_areas(roi_idx));
    avg_field_roi_normalE = sum(field_normalE.data(roi_idx) .*
nodes_areas(roi_idx))/sum(nodes_areas(roi_idx));

    struct = setfield(struct, {ii}, config, avg_field_roi_normalE)
    txt = sprintf('%s_electric_field_ROI.txt',sub);                % name textfile
to print results

    path = fullfile(pts, sub, std_config, 'subject_overlays', txt); % location for
textfile
    fid = fopen(path,'wt');       % file ID, where to file the printed text
    fprintf(fid, 'Subject: %s - The normE and normalE at ROI\n\n', sub);
    fprintf(fid, 'ROI is a sphere with %g mm radius at coordinates [ %g, %g,
%g]\n', r, target(1), target(2), target(3));
    fprintf(fid, 'mean %s in ROI: %f V/m\n', field_name_normE,
avg_field_roi_normE);
    fprintf(fid, 'mean %s in ROI: %f V/m\n', field_name_normalE,
avg_field_roi_normalE);

end
```

Published with MATLAB® R2020a

E. Changed SimNIBS source code

The subject-specific head models were made with SimNIBS (Saturnino et al., 2018; Thielscher et al., 2015) as described by (Piastra et al., 2021). In this process, SimNIBS also creates surface files (.GII) of the middle layer of the grey matter, these files are used for optimization in the normal E direction. These files can be found in the folder m2m_<SubjectID>\segment\cat\surf. These surface files are not included in the re-labelling process as described by (Piastra et al., 2021). Therefore, we have written a MATLAB function to include the lesion in these surface files (See Appendix D, Gifti2mesh_lesion). With this function, we create a surface mesh of the middle layer of the grey matter, based on these .GII files. In this mesh, we relabel the elements that are lesion.

To include this relabelled surface mesh in the optimization process, instead of the .GII surface files, we had to adjust the python source code of SimNIBS. The script we adjusted is:

C:\Users\<USERNAME>\SimNIBS-3.2\simnibs_env\Lib\site-packages\simnibs\simulation\sim_struct.py.

This script exists of multiple classes. In the class TDCSLEADFIELD(LEADFIELD), in the definition run:

```
1 def run(self, cpus=1, allow_multiple_runs=False, save_mat=True):
2 ''' Runs the calculations for the leadfield
3
4 Parameters
5 ----------
6 cpus: int (optional)
7 Number of cpus to use. Not nescessaraly will use all cpus.←-Default:1
8 allow_multiple_runs: bool (optinal)
9 Whether to allow multiple runs in one folder. Default: False
10 save_mat: bool (optional)
11 Whether to save the ".mat" file of this structure 12
13 Returns
14 ---------
15 Writes the simulations
16
17 '''
18 self._set_logger()
19 dir_name = os.path.abspath(os.path.expanduser(self.pathfem))
20 if os.path.isdir(dir_name):
21    g = glob.glob(os.path.join(dir_name, 'simnibs_simulation*.mat'←- ))
22    if len(g) > 0 and not allow_multiple_runs:
23          raise IOError(
24          '\nFound already existing simulation results in ←-
directory.'
25          '\nPlease run the simulation in a new directory or ←- delete'
26          ' the simnibs_simulation*.mat files from the folder : ←-
 {0}'.format(dir_name))
27    logger.info(
28    'Running simulations in the directory: {0}'.format(←-
dir_name))
29 else:
30 logger.info('Running simulations on new directory: {0}'.←-
dir_name)
```

```
31 os.makedirs(dir_name)
32
33 self._prepare()
34 if save_mat:
35 save_matlab_sim_struct(
36 self,
37 os.path.join(
38 dir_name,
39 'simnibs_simulation_{0}.mat'.format(self.time_str)) 40 )
41 # For simulations without electrodes
42 has_electrodes = self.electrode is not None
43 # Set electrode positions
44 if self.eeg_cap is not None:
45 if os.path.isfile(self.eeg_cap):
46 self._add_electrodes_from_cap()
47 else:
48 raise IOError(
49 'Could not find EEG cap file: {0}'.format(self.eeg_cap←- ))
50 try:
51 len(self.electrode)
52 except TypeError:
53 raise ValueError(
54 'Please define either an EEG cap or a list of electrodes') 55
56 for el in self.electrode:
57 if len(el.thickness) == 3:
58 raise ValueError('Can not run leadfield on sponge ←-
electrodes')
59 # Handle the ROI
60 if np.any(np.array(self.tissues) > 1000) and np.any(np.array(self.←-
tissues) < 1000):
61 raise ValueError('Mixing Volumes and Surfaces in ROI!') 62
63 if self.map_to_surf:
64 if np.any(np.array(self.tissues) < 1000):
65 raise ValueError("Can't combine volumetric ROI with ←- map_to_surf!")


66 roi = self.tissues + [2]
67 else:
68 roi = self.tissues
69
70 # Field of interest
71 if self.field != 'E' and self.field != 'J':
72 raise ValueError("field parameter should be E or J. "
73 "found: {0}".format(self.field))
74
75 self._add_el_conductivities()
76
77 # Get names for leadfield and file of head with cap
```

```
78 fn_hdf5 = os.path.join(dir_name, self._lf_name())
79 fn_el = os.path.join(dir_name, self._el_name())
80 if has_electrodes:
81 # Place electrodes
82 logger.info('Placing Electrodes')
83 w_elec, electrode_surfaces = self._place_electrodes()
84 mesh_io.write_msh(w_elec, fn_el)
85 scalp_electrodes = w_elec.crop_mesh([1005] + ←-
electrode_surfaces)
86 scalp_electrodes.write_hdf5(fn_hdf5, 'mesh_electrodes/')
87 input_type = 'tag'
88 else:
89 # Find the closest surface node
90 w_elec = self.mesh
91 out_nodes = np.unique(self.mesh.elm.get_outside_faces())
92 out_nodes_kdt = scipy.spatial.cKDTree(self.mesh.nodes[←-
out_nodes])
93 electrode_surfaces = []
94 for el in self.electrode:
95 _, idx = out_nodes_kdt.query(el.centre)
96 electrode_surfaces.append(out_nodes[idx])
97 # Update the position of the electrode
98 el.centre = self.mesh.nodes[electrode_surfaces[-1]]
99 mesh_io.write_geo_spheres(
100 [el.centre for el in self.electrode],
101 fn_el[:-4] + '.geo'
102 )
103 input_type = 'node'
104
105 # Write roi, scalp and electrode surfaces hdf5
106 roi_msh = w_elec.crop_mesh(roi)
107 # If mapping to surface
108 if self.map_to_surf:
109 # Load middle gray matter
110 s_names, segtype = \
111 transformations.get_surface_names_from_folder_structure(←-
self.subpath)
112 middle_surf = {}
113 if segtype == 'mri2mesh':
114 for hemi in ['lh', 'rh']:
115 wm_surface = mesh_io.read_freesurfer_surface(
116         s_names[hemi + '_wm'])
117 gm_surface = mesh_io.read_freesurfer_surface(
118         s_names[hemi + '_gm'])
119 middle_surf[hemi] = mesh_io._middle_surface(
120         wm_surface, gm_surface, .5)
121
122 elif segtype == 'headreco':
123 for i, hemi in enumerate(['lh', 'rh']):
124 # following lines added by Renee Dooren
```

```
125 logger.info('use of: middle_surf loop of TDCSLEADFIELD←- in
sim_struct')
126 mesh_for_ROI = "%s\mesh_midgm_with_lesion.msh" %(self.←- subpath) #
load gifti-mesh with correct labels
127 mesh_lf = mesh_io.read_msh(mesh_for_ROI)
128
129 hemi_name = "%s\%s_midgm_with_lesion.msh" %(self.←- subpath,hemi) #
load from m2m_folder the mesh ←-
                            created with gifti2mesh
130 middle_surf[hemi] = mesh_io.read_msh(hemi_name)
131 #middle_surf[hemi] = mesh_io.read_gifti_surface(
132 #       s_names[hemi + '_midgm']) # ORIGINAL LINE
133 middle_surf[hemi].elm.tag1 = (i + 1) * np.ones(
134 middle_surf[hemi].elm.nr, dtype=int) # ORIGINAL ←- LINE
135 middle_surf[hemi].elm.tag2 = (i + 1) * np.ones(
136 middle_surf[hemi].elm.nr, dtype=int) #ORIGINAL ←- LINE
137
138 #mesh_lf = middle_surf['lh'].join_mesh(middle_surf['rh']) # ←-
ORIGINAL LINE
139 if len(self.tissues) > 0:
140 try:
141 mesh_lf = mesh_lf.join_mesh(roi_msh.crop_mesh(self.←- tissues))
142 except ValueError:
143 logger.warning(f'Could not find tissues number {self.←- tissues}')
144
145 # Create interpolation matrix
146 M = roi_msh.interp_matrix(
147         mesh_lf.nodes.node_coord,
148         out_fill='nearest',
149         element_wise=True
150   )
151 # Define postprocessing operation
152 def post(out_field, M):
153 return M.dot(out_field)
154
155 post_pro = functools.partial(post, M=M)
156
157 else:
158 mesh_lf = roi_msh
159 post_pro = None
160
161 fn_roi = os.path.join(dir_name, self._mesh_roi_name())
162 mesh_lf.write(fn_roi)
163 mesh_lf.write_hdf5(fn_hdf5, 'mesh_leadfield/')
164 # Write information about number of nodes in left hemishere for ←-
compatibility
165 # with MNE
166 if self.map_to_surf:
167 with h5py.File(fn_hdf5, 'a') as f:
168 f['mesh_leadfield'].attrs['nodes_lh'] = middle_surf['lh'].←- nodes.nr
```

```
169 f['mesh_leadfield'].attrs['tr_lh'] = middle_surf['lh'].elm←- .nr
170
171 # Run Leadfield
172 dset = 'mesh_leadfield/leadfields/tdcs_leadfield'
173 logger.info('Running Leadfield')
174
175 c = SimuList.cond2elmdata(self, w_elec)
176         fem.tdcs_leadfield(
177         w_elec, c, electrode_surfaces, fn_hdf5,dset,
178         current=1., roi=roi,
179         post_pro=post_pro, field=self.field,
180         solver_options=self.solver_options,
181         n_workers=cpus,
182         input_type=input_type
183   )
184
185 with h5py.File(fn_hdf5, 'a') as f:
186 f[dset].attrs['electrode_names'] = [el.name.encode() for el in←-
self.electrode]
187 f[dset].attrs['reference_electrode'] = self.electrode[0].name 188
f[dset].attrs['electrode_pos'] = [el.centre for el in self.←-
                    electrode]
189 f[dset].attrs['electrode_cap'] = self.eeg_cap.encode() if self←-
.eeg_cap is not None else 'none'
190 f[dset].attrs['electrode_tags'] = electrode_surfaces
191 f[dset].attrs['tissues'] = self.tissues
192 f[dset].attrs['field'] = self.field
193 f[dset].attrs['current'] = '1A'
194 if self.field == 'E':
195 f[dset].attrs['units'] = 'V/m'
196 elif self.field == 'J':
197 f[dset].attrs['units'] = 'A/m2'
198 else:
199 f[dset].attrs['units'] = 'Au'
200 if self.map_to_surf:
201 f[dset].attrs['d_type'] = 'node_data'
202 f[dset].attrs['mapped_to_surf'] = 'True' 203 else:
204 f[dset].attrs['d_type'] = 'element_data' 205
f[dset].attrs['mapped_to_surf'] = 'False' 206
207 logger.info('=====================================')
208 logger.info('SimNIBS finished running leadfield') 209
logger.info('Final HDF5 file:')
210 logger.info(fn_hdf5)
211 logger.info('=====================================')
212 self._finish_logger()
```

F. Visualized results in the functional targets of two stroke subjects.

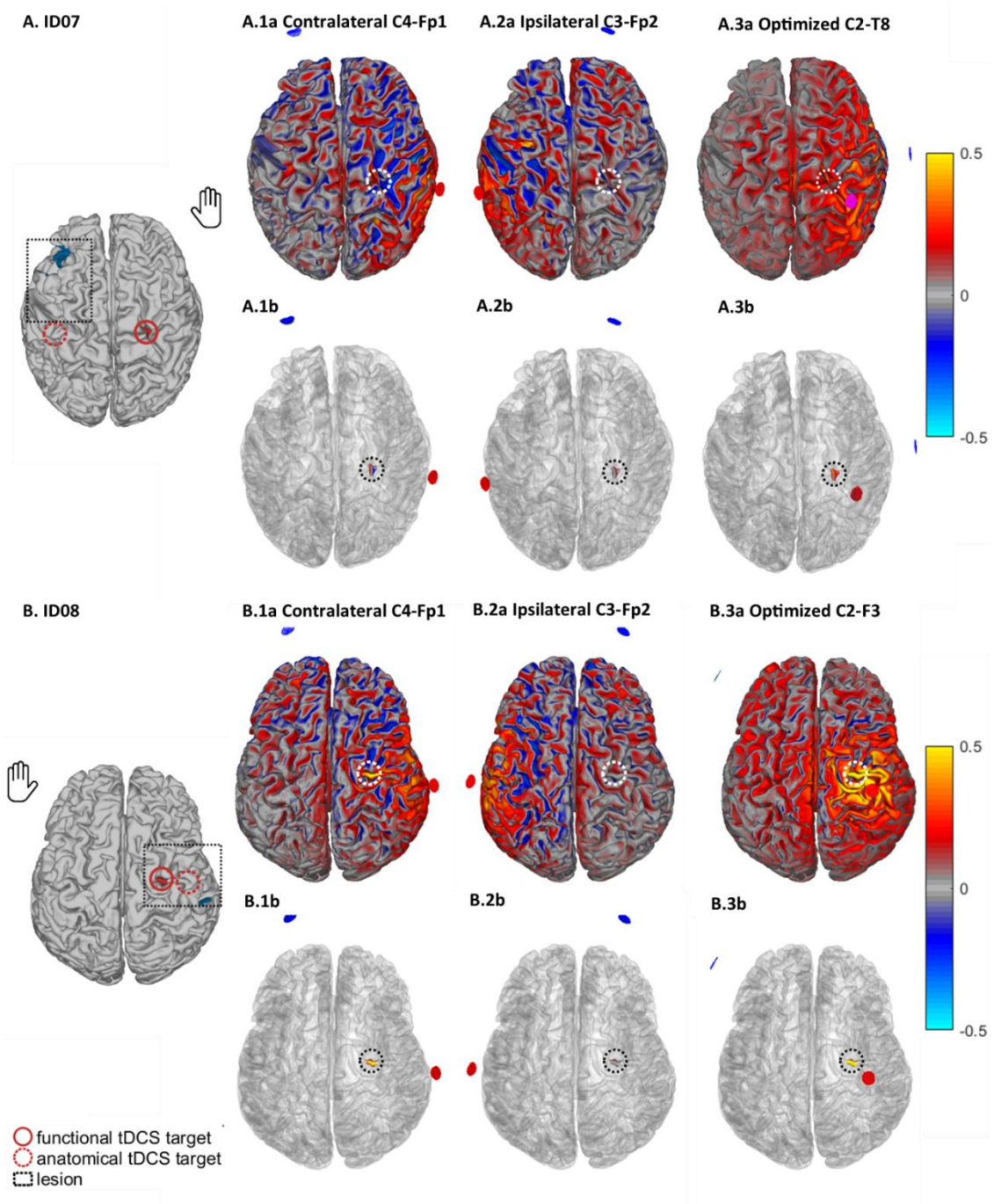

Figure 8. Visualized results in the functional targets of two stroke subjects. The mesh is showing the middle layer of the grey matter. In A. and B., an overview of the subjects' anatomy is shown; the functional tDCS target is indicated with a red circle, the anatomical tDCS target with a dashed line circle. The outer borders of the lesion are indicated with a black dashed rectangle. The functional target was found ipsilateral for ID07 and contralateral for ID08. The upper panel per subject (1a-3a) shows the E normal electric field distribution after stimulation throughout the brain, with the functional target indicated by the white dashed circle. The lower panel (1b-3b) show the field strength at the functional target. The colours of the field strength at the target may differ from the upper panel since the target may not be located on the surface of the cortex: in the lower panel, only the E-normal component of the target is shown. A.1, B1: the contralateral conventional configuration, A.2, B.2: the ipsilateral conventional configuration, A.3, B.3: the individual optimized configurations. Red and yellow represent a positive E normal, and blue and cyan represent a negative E normal. The anodes are presented in red, and the cathodes in blue.

G. Visualized results in the anatomical targets of two stroke subjects.

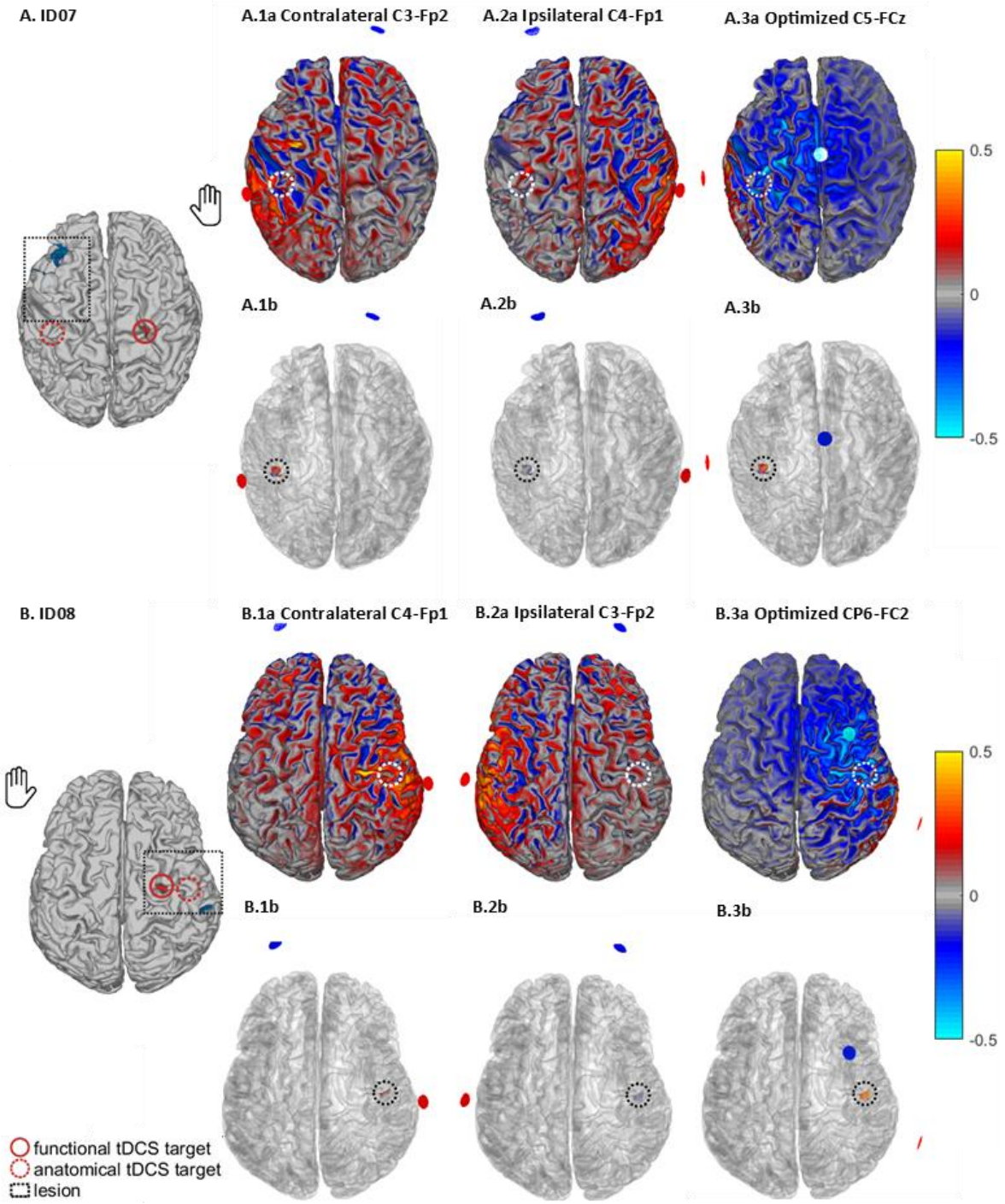

Figure 9. Visualized results in the anatomical targets of two stroke subjects. The mesh is showing the middle layer of the grey matter. In A. and B., an overview of the subjects' anatomy is shown; the functional tDCS target is indicated with a red circle, the anatomical tDCS target with a dashed line circle. The outer borders of the lesion are indicated with a black dashed rectangle. The upper panel per subject (1a-3a) shows the E normal electric field distribution after stimulation throughout the brain, with the anatomical target indicated by the white dashed circle. The lower panel (1b-3b) show the field strength at the anatomical target. The colours of the field strength at the target may differ from the upper panel since the target may not be located on the surface of the cortex: in the lower panel, only the E-normal component of the target is shown. A.1, B1: the contralateral conventional configuration, A.2, B.2: the ipsilateral conventional configuration, A.3, B.3: the individual optimized configurations. Red and yellow represent a positive E normal, and blue and cyan represent a negative E normal. The anodes are presented in red, and the cathodes in blue.